SECOND MOMENT FORMULAE FOR GEOMETRIC SAMPLING WITH TEST PROBES

(Running title: **Second moments for geometric sampling**)

Florian Voss and Luis M. Cruz–Orive

Corresponding author:
Professor Luis M. Cruz–Orive,
Departamento de Matemáticas, Estadística
y Computación,
Facultad de Ciencias,
Universidad de Cantabria,
Avda. Los Castros s/n,
E–39005 SANTANDER, Spain

Tel.: + 34 942 20 14 24
Fax: + 34 942 20 14 02
E-mail: Lcruz@matesco.unican.es

11050 words, 14 figures, 0 tables

SECOND MOMENT FORMULAE FOR GEOMETRIC SAMPLING WITH TEST PROBES

FLORIAN VOSS[1] and LUIS M. CRUZ-ORIVE[2]

[1]*Institute of Stochastics, Faculty of Mathematics and Economics, Ulm University, D-89069 Ulm, and* [2]*Department of Mathematics, Statistics and Computation, Faculty of Sciences, University of Cantabria, E-39005 Santander*

SUMMARY

First moment formulae for the intersection between a fixed geometric object and one moving according to the kinematic density constitute the basis of stereology and they are essentially well known. The corresponding second moment formulae are less known, however; some of them are scattered in the literature, and their proofs are often absent. Such formulae may be useful to compute exact variances when the objects involved have a known geometric shape on the one hand, and to obtain practical predictors of the estimation variance on the other. The purpose of this paper is to present a partly new, coherent set of second moment formulae for a fixed compact set intersected by mobile flats, bounded probes, or test systems endowed with the corresponding invariant measures, or by a stationary manifold process. We thereby contribute to a better understanding of the so called variance 'paradoxes', arising when a probe performs better than a higher dimensional one. For completeness we include the necessary tools in two appendixes.

Keywords: Flat, geometric covariogram, integral geometry, invariant density, Jensen-Gundersen paradoxes, kinematic density, manifold process, Ohser paradoxes, Poisson process, Rao-Blackwell theorem, stereology, systematic sampling, test probe, test system, variance.

AMS Subject Classification 2000: Primary: 60D05; Secondary: 52A22, 53C65, 62D05, 62M30.

1. INTRODUCTION

Geometrical parameters such as volume, surface area, length, number of components, etc., of a physical structure are of interest in many disciplines. Such properties can in principle be estimated by intersecting the structure with a geometric probe which typically consists of test points, lines, planes, or slabs. If the structure is fixed and bounded, then the probe has to be endowed with a proper mechanism of randomness (Miles & Davy, 1976; Davy & Miles, 1977), whereas, if the structure can be regarded as a realization of a random set (Stoyan *et al.*, 1995), then the control of the probe may not have to

be that strict. The former design is termed 'design based', the latter 'model based'; the theory and methodology of such designs constitute the object of stereology (Weibel, 1979; Baddeley & Jensen, 2004; Howard & Reed, 2005).

The first order properties of the relevant intersection measures are relatively straightforward, and they constitute the well known 'fundamental equations of stereology' (Miles, 1972; Cruz–Orive, 2002, 2003). Such equations are identities relating the target parameters of the structure with the mathematical expectation of the corresponding intersection measures, whereby the estimation of the parameters becomes a relatively simple matter. The second order properties of the intersection measures, however, are in general nontrivial and therefore less known: this paper is devoted to the study of such properties.

Second order properties of random intersection measures may be used, for instance:

(i). To obtain suitable variance models which allow the estimation of the variance of a stereological estimator from a sample of data. Here we obtain second order results as prerequisites to obtain further variance predictors for systematic sampling. So far the best known cases refer to systematic sampling with test points and segments on the real axis (Gual Arnau & Cruz-Orive, 1998; Cruz-Orive, 2006). Much further work is needed for sampling on higher dimensions with systematic probes (Cruz-Orive, 1989; Kiêu & Mora, 2006; Gual-Arnau & Cruz-Orive, 2006, and references therein).

(ii). To assist machine vision, automatic object detection, etc., in problems like: which are the mean and the second moment of the area of the intersection between a square and a hitting disk moving uniformly at random? Or, more generally, how to compute the first two moments of the random measure of the intersection between a nonvoid compact set and a regular grid of test points, curves, or windows?

(iii). To explain the so called 'variance paradoxes' of stereology, one of which states that point probes such as the four corners of a square may be more precise than the square itself to estimate an area (Jensen & Gundersen, 1982; Baddeley & Cruz-Orive, 1995; Voss, 2005). In the model based case, counting the lines hitting a convex window is more precise than measuring the corresponding intersection length to estimate the mean length per unit area of completely random straight lines on the plane, namely of 'Poisson lines', (Ohser, 1990; Baddeley & Cruz-Orive, 1995; Schladitz, 1996, 1999, 2000; Voss, 2005).

Our first purpose is to present a coherent and relatively comprehensive set of second moment formulae of the type mentioned in (ii) above. Our design based results (Sections 2–4) concern a compact set of dimension n in $\mathbb{R}^n$, hit by a geometric probe, or by a regular lattice of probes (called a test system) of dimension $q = 0, 1, ..., n$, such that the relative position and orientation of object and probe are 'random' in a well defined sense. The basic concepts and tools, and the well known first order properties, are given

in Appendix A. The best known second order formulae correspond to independent probes for $q = 0, 1, n$, and they are scattered in the literature (e.g. Matérn, 1960, 1989; Enns & Ehlers, 1978; Kellerer, 1986). For the model based case we consider second moment results involving Poisson probes of dimension $q = 0, 1, ..., n$, bounded or unbounded, intersecting a bounded set of dimension n in $\mathbb{R}^n$, (Section 7). Here the more familiar results concern also the cases $q = 0, 1, n$, (Ripley, 1981; Kellerer, 1986; Stoyan *et al.*, 1998; Diggle, 2003). The necessary prerequisites are given in Appendix B.

Our second purpose is to deepen in the understanding of the 'variance paradoxes' mentioned in (iii) above, extending and simplifying the known results and presenting new insights and examples; we do this in Sections 5, 6 and 8 using the results obtained in the earlier sections.

To facilitate reading a list of notation is supplied in Appendix D.

2. INDEPENDENT $q-$FLAT PROBES HITTING A COMPACT SET OF DIMENSION n IN $\mathbb{R}^n$

Consider a compact set $Y \subset \mathbb{R}^n$ with $\dim(Y) = n$ hit by an IUR $q-$flat $L_q(z,t)$, $q = 1, 2, ..., n-1$, namely a $q-$flat endowed with the probability element given by Eq. (A.6). Then the mean intersection contents is given by Eq. (A.9). The latter expression alone is not suitable to estimate the contents $\nu_n(Y)$ directly because it contains the mean total projection $\mathbb{E}_t \nu_{n-q}(Y_t')$, which is generally unknown; as we shall see, this difficulty disappears with the use of test systems (Section 4). Conditioning on the hitting event '$\uparrow$' is assumed throughout.

2.1 Second moment formulae for the intersection between a $q-$flat and a compact set of dimension n in $\mathbb{R}^n$

Proposition 2.1 If a $q-$flat $L_q(z,t)$ is FUR hitting the set Y with a probability element given by Eq. (A.7), then,

$$\mathbb{E}\big(\nu_q^2(Y \cap L_q(z,t))|t\big) = \frac{1}{\nu_{n-q}(Y_t')} \int_{L_q(0,t)} k_Y(x)\, \nu_q(\mathrm{d}x), \quad t \in G_{q,n-q}, \tag{2.1}$$

where $k_Y(x)$ is the geometric covariogram of Y, see Eq. (A.33).

Proof. Throughout we use the technique of expressing $\nu_q^2(\cdot)$ as the product of two integrals over indicator functions, and then applying Fubini's theorem. We obtain,

$$\begin{aligned} &\nu_{n-q}(Y_t')\, \mathbb{E}\big(\nu_q^2(Y \cap L_q(z,t))|t\big) \\ &= \int_{L_{n-q}(0,t)} \nu_q^2(Y \cap L_q(z,t)) \nu_{n-q}(\mathrm{d}z) \\ &= \int_{L_{n-q}(0,t)} \nu_{n-q}(\mathrm{d}z) \int_{L_q(z,t)} 1_Y(x)\, \nu_q(\mathrm{d}x) \int_{L_q(z,t)} 1_Y(y)\, \nu_q(\mathrm{d}y). \end{aligned} \tag{2.2}$$

For each point $y \in L_q(z,t)$ there is a unique point $\widetilde{x} \in L_q(0,t)$ such that $x = y + \widetilde{x}$, see Fig. 1. Further, the Lebesgue measure ν_n can be decomposed into the product of ν_q on $L_q(0,t)$ times ν_{n-q} on $L_{n-q}(0,t)$. Therefore,

$$\begin{aligned}
&\nu_{n-q}(Y_t')\,\mathbb{E}\big(\nu_q^2(Y\cap L_q(z,t))|t\big)\\
&= \int_{L_{n-q}(0,t)} \nu_{n-q}(\mathrm{d}z) \int_{L_q(z,t)} 1_Y(y)\,\nu_q(\mathrm{d}y) \int_{L_q(0,t)} 1_Y(y+\widetilde{x})\,\nu_q(\mathrm{d}\widetilde{x})\\
&= \int_{L_q(0,t)} \nu_q(\mathrm{d}\widetilde{x}) \int_{\mathbb{R}^n} 1_Y(y)\,1_Y(y+\widetilde{x})\,\nu_n(\mathrm{d}y)\\
&= \int_{L_q(0,t)} k_Y(x)\,\nu_q(\mathrm{d}x).
\end{aligned} \tag{2.3}$$

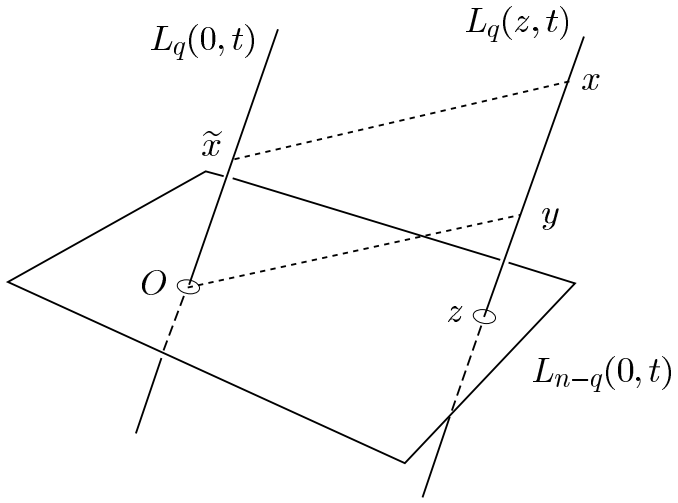

Figure 1 Construction used in the Lebesgue measure decomposition introduced in Subsection 2.1.

Corollary 2.1. If the $q-$flat is IUR hitting Y with a probability element given by Eq. (A.6), then,

$$\mathbb{E}\nu_q^2(Y\cap L_q(z,t)) = \frac{1}{\mathbb{E}_t\nu_{n-q}(Y_t')} \int_0^\infty q b_q r^{q-1} k_Y(r)\,\mathrm{d}r, \tag{2.4}$$

where $k_Y(r)$ is the isotropic covariogram of Y, see Eq. (A.36).

Proof. Take expectations on both sides of Eq. (2.1) with respect to the probability element given by Eq. (A.8), and recall the definition (A.36). We obtain,

$$\begin{aligned}
\mathbb{E}_t\nu_{n-q}(Y_t')\,\mathbb{E}\nu_q^2(Y\cap L_q(z,t)) &= \int_{G_{q,n-q}} \mathbb{P}(\mathrm{d}t) \int_{L_q(0,t)} k_Y(x)\,\nu_q(\mathrm{d}x)\\
&= \int_{L_q(0,0)} k_Y(\|x\|)\,\nu_q(\mathrm{d}x).
\end{aligned} \tag{2.5}$$

We may parametrize the point x by the spherical polar coordinates (r, u), whereby

$$\nu_q(\mathrm{d}x) = r^{q-1}\mathrm{d}u\,\mathrm{d}r,\ r \in (0,\infty),\ u \in \mathbb{S}^{q-1}, \tag{2.6}$$

and therefore,

$$\begin{aligned}\mathbb{E}_t\nu_{n-q}(Y_t')\,\mathbb{E}\nu_q^2(Y \cap L_q(z,t)) &= \int_{\mathbb{S}^{q-1}} \mathrm{d}u \int_0^\infty r^{q-1}k_Y(r)\,\mathrm{d}r \\ &= O_{q-1}\int_0^\infty r^{q-1}k_Y(r)\,\mathrm{d}r.\end{aligned} \tag{2.7}$$

2.2 **Example: convex set hit by a IUR straight line in $\mathbb{R}^2$.**

Consider a nonvoid convex set $Y \subset \mathbb{R}^2$ hit by an IUR straight line $L_1(z,t)$ in the same plane. Applying in turn Corollary 2.1 and Cauchy's projection formula (Eq. (A.11)), we obtain,

$$\begin{aligned}\mathbb{E}\nu_1^2(Y \cap L_1(z,t)) &= \frac{1}{\mathbb{E}_t\nu_1(Y_t')}\int_0^\infty 2k_Y(r)\,\mathrm{d}r \\ &= \frac{2\pi}{\nu_1(\partial Y)}\int_0^\infty k_Y(r)\,\mathrm{d}r.\end{aligned} \tag{2.8}$$

The preceding integral is finite because the set Y is bounded.

Disk hit by a IUR straight line in $\mathbb{R}^2$. Suppose that Y is a disk of diameter d in the plane. Substituting Eq. (A.37) into the right hand side of Eq. (2.8) we get,

$$\mathbb{E}\nu_1^2(Y \cap L_1(z,t)) = \frac{2}{d}\int_0^d k_{disk}(r,d)\,\mathrm{d}r = \frac{2}{3}d^2. \tag{2.9}$$

Square hit by a IUR straight line in $\mathbb{R}^2$. Let Y represent a square of side length s in the plane. Substituting Eq. (A.38) into the right hand side of Eq. (2.8) we get,

$$\begin{aligned}\mathbb{E}\nu_1^2(Y \cap L_1(z,t)) &= \frac{2\pi}{4s}\left[\int_0^s k_{sq,1}(r,s)\,\mathrm{d}r + \int_s^{s\sqrt{2}} k_{sq,2}(r,s)\,\mathrm{d}r\right] \\ &= \left(\log\left(1+\sqrt{2}\right) + \left(1-\sqrt{2}\right)/3\right)s^2.\end{aligned} \tag{2.10}$$

Remark 2.1. From Eq. (2.4) it is easy to show that, in general,

$$\mathbb{E}\nu_q^2(Y \cap L_q(z,t)) = (\text{shape constant}) \cdot (\text{scale factor})^{2q}. \tag{2.11}$$

3. INDEPENDENT BOUNDED $q-$PROBES HITTING A COMPACT SET OF DIMENSION n IN $\mathbb{R}^n$

Consider a compact set $Y \subset \mathbb{R}^n$ with $\dim(Y) = n$ hit by a bounded IUR $q-$probe $T_{z,t}$ with $\dim(T_{0,0}) = q$, $q = 0, 1, ..., n$, namely a $q-$probe endowed with the probability element given by Eq. (A.18). Then the mean intersection contents is given by Eq. (A.21), and analogous remarks apply to those made in Section 2 regarding the direct applicability of the latter expression, because Eq. (A.21) depends on the mean Minkowski addition $\mathbb{E}_t\nu_n(Y \oplus \breve{T}_{0,t})$. Next we study the second moment measures.

3.1 Second moment formulae for the intersection between a bounded probe of dimension q and a compact set of dimension n in $\mathbb{R}^n$

Proposition 3.1. If a bounded $q-$probe $T_{z,t}$ is FUR hitting the set Y with the uniform probability element given by Eq. (A.19), then,

$$\mathbb{E}\big(\nu_q^2(Y \cap T_{z,t})|t\big) = \frac{1}{\nu_n\big(Y \oplus \breve{T}_{0,t}\big)} \int_{T_{0,0}} \int_{T_{0,0}} k_Y(y-x)\, \nu_q(\mathrm{d}x)\, \nu_q(\mathrm{d}y), \quad t \in G_{n[0]}, \tag{3.1}$$

where $k_Y(x)$ is the geometric covariogram of Y.

Proof. Regard the set $Y := Y_{z,t}$ as mobile hitting the fixed $q-$probe $T_{0,0}$ with the uniform probability element given by Eq. (A.19). Then,

$$\begin{aligned}
&\nu_n\big(Y \oplus \breve{T}_{0,t}\big)\, \mathbb{E}\big(\nu_q^2(Y \cap T_{z,t})|t\big) \\
&= \int_{\mathbb{R}^n} \nu_q^2(T_{0,0} \cap Y_{z,t})\, \nu_n(\mathrm{d}z) \\
&= \int_{\mathbb{R}^n} \nu_n(\mathrm{d}z) \int_{T_{0,0}} 1_{Y_{z,t}}(x)\, \nu_q(\mathrm{d}x) \int_{T_{0,0}} 1_{Y_{z,t}}(y)\, \nu_q(\mathrm{d}y) \\
&= \int_{T_{0,0}} \nu_q(\mathrm{d}x) \int_{T_{0,0}} \nu_q(\mathrm{d}y) \int_{\mathbb{R}^n} 1_{Y_{-x,t}}(-z)\, 1_{Y_{-x,t}}(-z+y-x)\, \nu_n(\mathrm{d}z) \\
&= \int_{T_{0,0}} \int_{T_{0,0}} k_Y(y-x)\, \nu_q(\mathrm{d}x)\, \nu_q(\mathrm{d}y).
\end{aligned} \tag{3.2}$$

Corollary 3.1. If the $q-$probe is IUR hitting Y with the probability element given by Eq. (A.18), then,

$$\mathbb{E}\nu_q^2(Y \cap T_{z,t}) = \frac{1}{\mathbb{E}_t\nu_n\big(Y \oplus \breve{T}_{0,t}\big)} \int_{T_{0,0}} \int_{T_{0,0}} k_Y\big(\|y-x\|\big)\, \nu_q(\mathrm{d}x)\, \nu_q(\mathrm{d}y), \tag{3.3}$$

where $k_Y(r)$ is the isotropic covariogram of Y, see Eq. (A.36).

Proof. Take expectations on both sides of Eq. (3.1) with respect to the probability element given by Eq. (A.20).

3.2 **Special case of a '$q-$plate probe'**

Proposition 3.2. Suppose that the $q-$probe $T_{0,0}$ is a '$q-$plate', namely a bounded $q-$dimensional subset of a linear subspace $L_q(0,0)$, $q=1,2,...,n$. If $T_{z,t}$ is FUR hitting the set Y with a probability element given by Eq. (A.19), then,

$$\mathbb{E}\big(\nu_q^2(Y\cap T_{z,t})|t\big)=\frac{1}{\nu_n\big(Y\oplus\breve{T}_{0,t}\big)}\int_{L_q(0,t)}k_Y(z)\,k_{T_{0,t}}(z)\,\nu_q(\mathrm{d}z)\,,\quad t\in G_{n[0]},\tag{3.4}$$

where $k_Y(x)$ is the geometric covariogram of Y in $\mathbb{R}^n$, whereas $k_{T_{0,t}}(x)$ is that of $T_{0,t}$ in $\mathbb{R}^q$, namely within its containing linear $q-$subspace $L_q(0,t)$.

Proof. We have,

$$\begin{aligned}&\nu_n\big(Y\oplus\breve{T}_{0,t}\big)\,\mathbb{E}\big(\nu_q^2(Y\cap T_{z,t})|t\big)\\&=\int_{\mathbb{R}^n}\nu_n(\mathrm{d}z)\int_{L_q(z,t)}\int_{L_q(z,t)}1_Y(x)\,1_{T_{z,t}}(x)\,1_Y(y)\,1_{T_{z,t}}(y)\,\nu_q(\mathrm{d}x)\;\nu_q(\mathrm{d}y).\end{aligned}\tag{3.5}$$

Set $y=x+\widetilde{y}$ and then use the decomposition $\nu_n(\mathrm{d}z)=\nu_q\big(\mathrm{d}z^{(q)}\big)\cdot\nu_{n-q}\big(\mathrm{d}z^{(n-q)}\big)$, where $z^{(q)}\in L_q(0,t)$, $z^{(n-q)}\in L_{n-q}(0,t)$, $q=0,1,...,n$. We obtain,

$$\begin{aligned}&\nu_n\big(Y\oplus\breve{T}_{0,t}\big)\,\mathbb{E}\big(\nu_q^2(Y\cap T_{z,t})|t\big)\\&=\int\limits_{L_q(0,t)}\nu_q\big(\mathrm{d}z^{(q)}\big)\int\limits_{L_{n-q}(0,t)}\nu_{n-q}\big(\mathrm{d}z^{(n-q)}\big)\\&\times\int\limits_{L_q(z^{(n-q)},t)}\int\limits_{L_q(0,t)}1_Y(x)\,1_Y(x+\widetilde{y})\,1_{T_{0,t}}(x-z)1_{T_{0,t}}(x-z+\widetilde{y})\,\nu_q(\mathrm{d}\widetilde{y})\,\nu_q(\mathrm{d}x)\\&=\int\limits_{L_{n-q}(0,t)}\nu_{n-q}\big(\mathrm{d}z^{(n-q)}\big)\int\limits_{L_q(z^{(n-q)},t)}\int\limits_{L_q(0,t)}1_Y(x)\,1_Y(x+\widetilde{y})\\&\times\int\limits_{L_q(0,t)}1_{T_{0,t}}(x-z)1_{T_{0,t}}(x-z+\widetilde{y})\,\nu_q\big(\mathrm{d}z^{(q)}\big)\,\nu_q(\mathrm{d}\widetilde{y})\,\nu_q(\mathrm{d}x)\\&=\int\limits_{L_q(0,t)}k_{T_{0,t}}(\widetilde{y})\,\nu_q(\mathrm{d}\widetilde{y})\int\limits_{L_{n-q}(0,t)}\int\limits_{L_q(z^{(n-q)},t)}1_Y(x)\,1_Y(x+\widetilde{y})\,\nu_q(\mathrm{d}x)\,\nu_{n-q}\big(\mathrm{d}z^{(n-q)}\big)\\&=\int\limits_{L_q(0,t)}k_Y(\widetilde{y})\,k_{T_{0,t}}(\widetilde{y})\,\nu_q(\mathrm{d}\widetilde{y}).\end{aligned}\tag{3.6}$$

Corollary 3.2. If the bounded $q-$plate probe $T_{z,t}$ is IUR hitting Y with the probability element given by Eq. (A.18), then,

$$\mathbb{E}\nu_q^2(Y \cap T_{z,t}) = \frac{1}{\mathbb{E}_t \nu_n\big(Y \oplus \breve{T}_{0,t}\big)} \int_0^\infty q b_q r^{q-1} k_Y(r)\, k_{T_{0,0}}(r)\, \mathrm{d}r. \tag{3.7}$$

where $k_Y(r)$ is the isotropic covariogram of Y, whereas $k_{T_{0,0}}(r)$ is the isotropic covariogram of $T_{0,0}$ within its containing linear subspace $L_q(0,0)$.

Proof. Take expectations on both sides of Eq. (3.4) with respect to the probability element (A.20) and obtain first the isotropic covariogram $k_Y(r)$. Then apply Eq. (2.6) and obtain the isotropic covariogram $k_{T_{0,t}}(r)$ bearing Eq. (A.35), (with $n = q$), in mind.

Remark 3.1. It should be stressed that Eq. (3.4), (3.7) hold if $T_{0,0}$ is of full dimension q within $L_q(0,0)$. For instance, if $q = 1$ then $T_{0,0}$ may be a straight line segment, whereas if $q = 2$ then $T_{0,0}$ may be a platelet, but not a planar curve.

Remark 3.2. In the literature, the best known results in the present context correspond to Eq. (3.3) with $q = 0, n$.

3.3 Examples for $n = 2$.

We present five examples with a double purpose, namely to illustrate the foregoing propositions in the first place, and then to obtain the results which will be used in Subsections 5.3, 5.4. The first example illustrates Eq. (3.7) with $q = n = 2$. The second, third, and fourth examples refer to 1–dimensional probes, namely $q = 1$, $n = 2$; however, whereas in the second example Eq. (3.7) may be used, in the third and fourth ones we have to resort to Eq. (3.3) directly. Finally, the fifth example illustrates the case $q = 0$, $n = 2$, which uses Eq. (3.3) as well.

Here, and in the rest of the paper, we do not display the explicit expressions of the integrals involved (whenever available), first because they are not particularly illuminating, and second because they can be computed readily with a suitable mathematical package. For the relevant plots we extensively used the command `NIntegrate[]` from MATHEMATICA®.

Probe of dimension $q = 2$: disk hit by a square. Let $Y \subset \mathbb{R}^2$ represent a disk of diameter d and $T_{0,0} \subset \mathbb{R}^2$ a square probe of side length s. If $T_{z,t}$ is IUR hitting Y, then Eq. (3.7) yields,

$$\mathbb{E}\nu_2^2(Y \cap T_{z,t}) = \frac{1}{\mathbb{E}_t \nu_2\big(Y \oplus \breve{T}_{0,t}\big)} \int_0^\infty 2\pi r k_Y(r)\, k_{T_{0,0}}(r)\, \mathrm{d}r. \tag{3.8}$$

The denominator in the right hand side of the preceding expression is directly available from Eq. (A.23), namely,

$$\mathbb{E}_t \nu_2\big(Y \oplus \breve{T}_{0,t}\big) = \pi d^2/4 + s^2 + 2sd, \tag{3.9}$$

whereas the geometric covariograms $k_Y(r)$ and $k_{T_{0,0}}(r)$ are given by Eq. (A.37) and Eq. (A.38) respectively. We obtain,

$$(2\pi)^{-1}\mathbb{E}_t \nu_2\big(Y \oplus \breve{T}_{0,t}\big) \cdot \mathbb{E}\nu_2^2(Y \cap T_{z,t})$$

$$= \begin{cases} \displaystyle\int_0^s r k_{disk}(r,d)\, k_{sq,1}(r,s)\,\mathrm{d}r + \int_s^{s\sqrt{2}} r k_{disk}(r,d)\, k_{sq,2}(r,s)\,\mathrm{d}r\,, & \big(0 \le s \le d/\sqrt{2}\big), \\ \displaystyle\int_0^s r k_{disk}(r,d)\, k_{sq,1}(r,s)\,\mathrm{d}r + \int_s^{d} r k_{disk}(r,d)\, k_{sq,2}(r,s)\,\mathrm{d}r\,, & \big(d/\sqrt{2} < s \le d\big), \\ \displaystyle\int_0^d r k_{disk}(r,d)\, k_{sq,1}(r,s)\,\mathrm{d}r, & (d < s < \infty). \end{cases} \tag{3.10}$$

As $s \to \infty$ the square will contain the disk with probability 1, and from the first of the preceding equations it can be verified that $\mathbb{E}\nu_2^2(Y \cap T_{z,t})$ converges to $\big(\pi d^2/4\big)^2$, as expected.

Probe of dimension $q = 1$: disk hit by a straight line segment. Consider a disk $Y \subset \mathbb{R}^2$ of diameter d and a straight line segment $T_{0,0} \subset \mathbb{R}^2$ of length l, see Fig. 2(a). If $T_{z,t}$

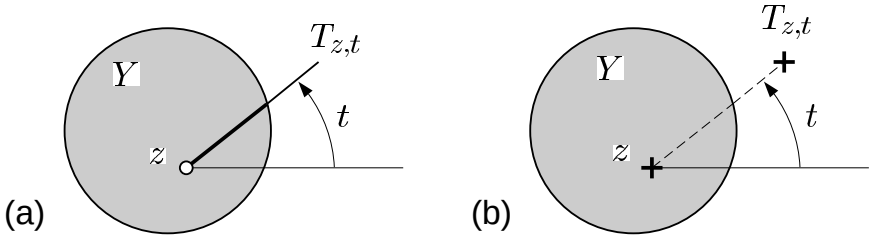

Figure 2 Fixed disk hit by a straight line segment probe (a) and with a pair of test points (b) equipped with the kinematic measure in the plane.

is IUR hitting Y, then Eq. (3.7) applies. Making use of Eq. (A.37) and (A.39) we obtain,

$$\mathbb{E}_t \nu_2\big(Y \oplus \breve{T}_{0,t}\big) \cdot \mathbb{E}\nu_1^2(Y \cap T_{z,t}) = \int_0^\infty 2 k_Y(r)\, k_{T_{0,0}}(r)\,\mathrm{d}r$$

$$= \begin{cases} 2\int_0^l k_{disk}(r,d) \cdot (l-r)\,\mathrm{d}r, & (0 < l \le d), \\ 2\int_0^d k_{disk}(r,d) \cdot (l-r)\,\mathrm{d}r, & (d < l \le \infty), \end{cases} \tag{3.11}$$

where, in this case,

$$\mathbb{E}_t \nu_2\big(Y \oplus \breve{T}_{0,t}\big) = \pi d^2/4 + ld. \tag{3.12}$$

Logically as $l \to \infty$ the second moment converges to the right hand side of Eq. (2.9).

Probe of dimension $q = 1$: square hit by the boundary of a circle. Suppose now that the probe $T_{0,0} \subset \mathbb{R}^2$ is the boundary of a disk, namely a circle of diameter d hitting a square $Y \subset \mathbb{R}^2$ of side length s uniformly at random. Since the circle is not a subset of a straight line, we have to use Eq. (3.3) instead of Eq. (3.7), namely

$$\mathbb{E}\nu_1^2(Y \cap T_{z,t}) = \frac{1}{\mathbb{E}_t\nu_2\big(Y \oplus \breve{T}_{0,t}\big)} \int_{T_{0,0}} \int_{T_{0,0}} k_Y\big(\|y - x\|\big)\, \nu_1(\mathrm{d}x)\, \nu_1(\mathrm{d}y). \tag{3.13}$$

Consider a mobile point $x(l) \in T_{0,0}$, where l denotes the arc length from a fixed point $y \in T_{0,0}$ to $x(l)$, (Fig. 3). Then $\|y - x(l)\| = d \cdot \sin(l/d)$ and, recalling Eq. (A.38), Eq. (3.13) becomes,

$$\mathbb{E}_t\nu_2\big(Y \oplus \breve{T}_{0,t}\big) \cdot \mathbb{E}\nu_1^2(Y \cap T_{z,t}) = \int_{T_{0,0}} \nu_1(\mathrm{d}y) \int_0^{\pi d} k_Y\big(d \cdot \sin(l/d)\big)\, \mathrm{d}l. \tag{3.14}$$

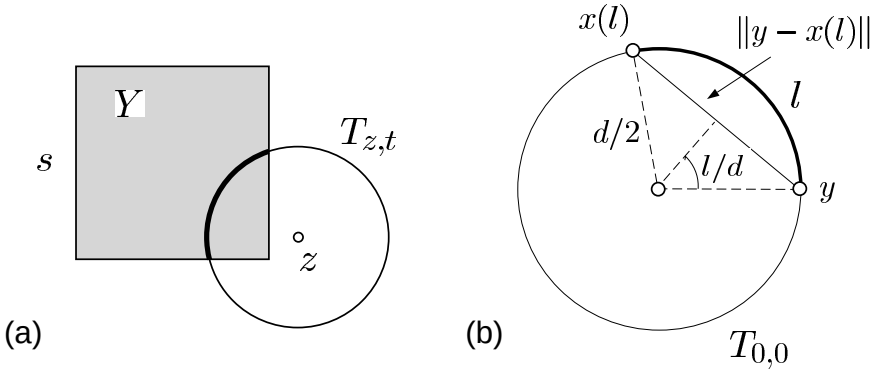

Figure 3 (a), square hit by a uniform random circle. (b), illustration of the relevant distance $\|y - x(l)\| = d\, \sin(l/d)$, see the example in Subsection 3.3.

Thus,

$$\begin{aligned}
&(\pi d)^{-1}\, \mathbb{E}_t\nu_2\big(Y \oplus \breve{T}_{0,t}\big) \cdot \mathbb{E}\nu_1^2(Y \cap T_{z,t}) \\
&= \begin{cases}
\int_0^{d\sin^{-1}(s/d)} k_{sq,1}(d \cdot \sin(l/d), s)\, \mathrm{d}l \\
+ \int_{d\sin^{-1}(s/d)}^{d\sin^{-1}\left(s\sqrt{2}/d\right)} k_{sq,2}(d \cdot \sin(l/d, s))\, \mathrm{d}l, & \big(0 \le s < d/\sqrt{2}\big), \\
\int_0^{d\sin^{-1}(s/d)} k_{sq,1}(d \cdot \sin(l/d), s)\, \mathrm{d}l, & \big(d/\sqrt{2} < s \le d\big), \\
\int_0^{\pi d} k_{sq,1}(d \cdot \sin(l/d), s)\, \mathrm{d}l, & (d < s < \infty).
\end{cases}
\end{aligned} \tag{3.15}$$

On the other hand,

$$\mathbb{E}_t\nu_2\big(Y \oplus \breve{T}_{0,t}\big) = \begin{cases} 2\big(\pi d^2/4 - k_{disk}(s,d)\big) + 2sd, & \big(0 < s < d/\sqrt{2}\big), \\ \pi d^2/4 + s^2 + 2sd, & \big(d/\sqrt{2} < s \le \infty\big) \end{cases} \tag{3.16}$$

For large d, series expansion of the first Eq. (3.16) yields,

$$4sd - s^3/(3d) + O\big(s^5/d^3\big), \;\; d \gg s. \tag{3.17}$$

On the other hand, as $s \to \infty$ the square will contain the circle with probability 1, and the second moment tends to $(\pi d)^2$, as expected.

Probe of dimension $q = 1$: square hit by the boundary of another square. Here the probe $T_{0,0} \subset \mathbb{R}^2$ is the boundary of a square of side length s hitting a fixed square $Y \subset \mathbb{R}^2$ of side length d isotropically and uniformly at random. Again $T_{0,0}$ is not a subset of a straight line, and therefore we have to use Eq. (3.13). Consider two points ξ, η on $T_{0,0}$, and let x, y denote the respective distances of each of these points from say the leftward, or the downward (as applicable) endpoint of the side containing the point, $(0 \le x, y \le s)$. Then the required distance $\|\xi - \eta\|$ is equal to $|x - y|$ if both points lie on the same side, to $\sqrt{x^2 + y^2}$ if they lie on adjacent sides, and to $\sqrt{(x-y)^2 + s^2}$ if they lie on opposite sides of the square probe. Therefore,

$$\begin{aligned}\mathbb{E}_t \nu_2\big(Y \oplus \breve{T}_{0,t}\big) \cdot \mathbb{E}\nu_1^2\big(Y \cap T_{z,t}\big) = 4 \int_0^s \Bigg[\int_0^s k_Y(|x-y|)\,\mathrm{d}y + 2\int_0^s k_Y\Big(\sqrt{x^2+y^2}\Big)\,\mathrm{d}y \\ + \int_0^s k_Y\Big(\sqrt{(x-y)^2 + s^2}\Big)\,\mathrm{d}y\Bigg]\,\mathrm{d}x.\end{aligned} \tag{3.18}$$

Depending on the relative sizes of s, d the preceding expression takes different forms. The details are given in Appendix C.1. Moreover,

$$\mathbb{E}_t \nu_2\big(Y \oplus \breve{T}_{0,t}\big) = \begin{cases} \frac{16}{\pi} sd - \frac{2}{\pi} s^2, & \big(0 < s \le d/\sqrt{2}\big), \\ \frac{16}{\pi} sd - \frac{2}{\pi} s^2 - \frac{6}{\pi} sd\sqrt{2 - \frac{d^2}{s^2}} & \\ \quad + \frac{4}{\pi}\big(d^2 + s^2\big)\cos^{-1}\Big(\frac{d}{s\sqrt{2}}\Big), & \big(d/\sqrt{2} < s \le d\big), \\ d^2 + s^2 + \frac{8}{\pi} sd, & (d < s < \infty). \end{cases} \tag{3.19}$$

Probe of dimension $q = 0$: disk hit by the vertices of a square. Consider a disk $Y \subset \mathbb{R}^2$ of diameter d hit uniformly at random with a 0–probe $T_{0,0} \subset \mathbb{R}^2$ consisting of the union of the four vertices $\{x_1, x_2, x_3, x_4\}$ of a square of side length s. The proper

choice, namely Eq. (3.3), reduces in this case to a double summation namely,

$$\begin{aligned}
&\mathbb{E}_t\nu_2\big(Y\oplus\breve{T}_{0,t}\big)\,\mathbb{E}\nu_0^2(Y\cap T_{z,t})\\
&=\sum_{i=1}^{4}\sum_{j=1}^{4}k_Y\big(\|x_i-x_j\|\big)\\
&=4k_Y(0)+8k_Y(s)+4k_Y\Big(s\sqrt{2}\Big)\\
&=\begin{cases}\pi d^2+8\,k_{disk}(s,d)+4\,k_{disk}\big(s\sqrt{2},d\big), & \big(0\le s\le d/\sqrt{2}\big)\\ \pi d^2+8\,k_{disk}(s,d), & \big(d/\sqrt{2}<s\le d\big),\\ \pi d^2, & (d<s<\infty).\end{cases}
\end{aligned}\tag{3.20}$$

On the other hand,

$$\mathbb{E}_t\nu_2\big(Y\oplus\breve{T}_{0,t}\big)=\begin{cases}\frac{3}{4}\pi d^2+s^2-2k_{disk}(s,d), & \big(0\le s\le d/\sqrt{2}\big),\\ \pi d^2-4k_{disk}(s,d) & \big(d/\sqrt{2}<s\le d\big),\\ \pi d^2 & (d<s\le\infty),\end{cases}\tag{3.21}$$

namely the area of the union of four disks of diameter d centred at the vertices of a square of side length s. As $s\to 0$ it is easily verified that $\mathbb{E}\nu_0^2(Y\cap T_{z,t})\to 16$, (naturally $\mathbb{P}\big(\nu_0\big(Y\cap\breve{T}_{z,t}\big)=4\big)\to 1$ as $s\to 0$).

4. TEST SYSTEMS OF $q-$PROBES HITTING A COMPACT SET OF DIMENSION n IN $\mathbb{R}^n$

Let $Y\subset\mathbb{R}^n$ represent a compact set with $\dim(Y)=n$ hit by an IUR test system $\Lambda_{z,t}$ with $\dim(\Lambda_{0,0})=q$, $q=0,1,...,n$, (see Appendix A.3), with the probability element given by Eq. (A.26). Then the mean intersection contents is given by Eq. (A.28). Note that the estimation problems raised in the introductory paragraphs of Sections 2, 3 disappear here because all the quantities in Eq. (A.28) except $\nu_k(Y_k)$ (which is assumed to be the target quantity), are either known or observable. For this reason the test systems considered here are fundamental tools in practical stereology.

In this section we extend to test systems the foregoing second order results pertaining to independent probes.

4.1 Second moment formulae for the intersection between a test system of bounded $q-$probes and a compact set of dimension n in $\mathbb{R}^n$

Proposition 4.1 If a test system $\Lambda_{z,t}$ of bounded $q-$probes is FUR hitting a compact set $Y\subset\mathbb{R}^n$ of dimension n with a probability element given by the second factor in the right hand side of Eq. (A.26), then,

$$\mathbb{E}\big(\nu_q^2(Y\cap\Lambda_{z,t})|t\big)=\frac{1}{\nu_n\big(J_{0,0}\big)}\int_{T_{0,t}}\int_{\Lambda_{0,t}}k_Y(y-x)\,\nu_q(\mathrm{d}x)\,\nu_q(\mathrm{d}y),\quad t\in G_{n[0]},\tag{4.1}$$

where $k_Y(x)$ is the geometric covariogram of Y.

Proof.

$$\begin{aligned}
&\nu_n\big(J_{0,0}\big)\,\mathbb{E}\big(\nu_q^2(Y\cap\Lambda_{z,t})|t\big)\\
&=\int_{J_{0,t}}\nu_q^2(T_{0,0}\cap\Lambda_{z,t})\,\nu_n(\mathrm{d}z)\\
&=\int_{J_{0,t}}\nu_n(\mathrm{d}z)\int_{\Lambda_{z,t}}1_Y(x)\,\nu_q(\mathrm{d}x)\int_{\Lambda_{z,t}}1_Y(y)\,\nu_q(\mathrm{d}y)\\
&=\int_{J_{0,t}}\nu_n(\mathrm{d}z)\int_{\Lambda_{0,t}}1_Y(x+z)\,\nu_q(\mathrm{d}x)\int_{\Lambda_{0,t}}1_Y(y+z)\,\nu_q(\mathrm{d}y)\\
&=\int_{J_{0,t}}\nu_n(\mathrm{d}z)\sum_{k\in\mathbb{Z}}\int_{T_{0,t}}1_Y(x+z+\tau_{k,t})\,\nu_q(\mathrm{d}x)\sum_{l\in\mathbb{Z}}\int_{T_{0,t}}1_Y(y+z+\tau_{l,t})\,\nu_q(\mathrm{d}y).
\end{aligned}\tag{4.2}$$

For each $k,l\in\mathbb{Z}$ there is a unique $j\in\mathbb{Z}$ such that $\tau_{k,t}=\tau_{l,t}+\tau_{j,t}$. Thus,

$$\begin{aligned}
&\nu_n\big(J_{0,0}\big)\,\mathbb{E}\big(\nu_q^2(Y\cap\Lambda_{z,t})|t\big)\\
&=\int_{T_{0,t}}\int_{T_{0,t}}\nu_q(\mathrm{d}x)\nu_q(\mathrm{d}y)\sum_{j\in\mathbb{Z}}\sum_{l\in\mathbb{Z}}\int_{J_{0,t}}1_{Y_{-y}}(z+\tau_{l,t}+x-y+\tau_{j,t})\,1_{Y_{-y}}(z+\tau_{l,t})\,\nu_n(\mathrm{d}z)\\
&=\int_{T_{0,t}}\int_{T_{0,t}}\sum_{j\in\mathbb{Z}}k_Y(x-y+\tau_{j,t})\,\nu_q(\mathrm{d}x)\,\nu_q(\mathrm{d}y)\\
&=\int_{T_{0,t}}\int_{\Lambda_{0,t}}k_Y(y-x)\,\nu_q(\mathrm{d}x)\,\nu_q(\mathrm{d}y).
\end{aligned}\tag{4.3}$$

Corollary 4.1. If the test system $\Lambda_{z,t}$ of $q-$probes is IUR hitting Y with the probability element given by Eq. (A.26), then,

$$\mathbb{E}\nu_q^2(Y\cap\Lambda_{z,t})=\frac{1}{\nu_n\big(J_{0,0}\big)}\int_{T_{0,0}}\int_{\Lambda_{0,0}}k_Y(\|y-x\|)\,\nu_q(\mathrm{d}x)\,\nu_q(\mathrm{d}y),\tag{4.4}$$

where $k_Y(r)$ is the isotropic covariogram of Y, see Eq. (A.36).

Proof. First, take expectations on both sides of Eq. (4.1) with respect top the probability element given by the first factor in the right hand side of Eq. (A.26). Then, apply the inverse rotation t^{-1} to the set Y, whereby the domains of integration $T_{0,t},\Lambda_{0,t}$ become

$T_{0,0}, \Lambda_{0,0}$ respectively. Since the measure ν_q is rotation invariant, we obtain,

$$\begin{aligned}
&\nu_n\big(J_{0,0}\big)\,\mathbb{E}\nu_q^2(Y\cap\Lambda_{z,t})\\
&=\int_{T_{0,0}}\nu_q(\mathrm{d}y)\int_{\Lambda_{0,0}}\nu_q(\mathrm{d}x)\int_{G_{n\,[0]}}k_{Y_{0,t^{-1}}}(y-x)\,\mathbb{P}(\mathrm{d}t)\\
&=\int_{T_{0,0}}\nu_q(\mathrm{d}y)\int_{\Lambda_{0,0}}k_Y(\|y-x\|)\,\nu_q(\mathrm{d}x)\,.
\end{aligned}\tag{4.5}$$

4.2 **Special case of a test system of $q-$plates**

Here we extend the concept of $q-$plate probe introduced in Subsection 3.2 to test systems. To achieve this we restrict ourselves to test systems $\Lambda_{0,0}$ with fundamental 'box' tiles of the form

$$J_{0,0}=[0,a_1)\times[0,a_2)\times\cdots\times[0,a_n),\ a_i>0,\ i=1,2,...,n.\tag{4.6}$$

Further we assume that the fundamental probe is a $q-$dimensional bounded subset of a linear $q-$subspace, namely,

$$\begin{aligned}
&T_{0,0}\subset L_q(0,0),\ \dim(T_{0,0})=q,\ q=0,1,...,n,\\
&T_{0,0}\subset[0,a_1)\times[0,a_2)\times\cdots\times[0,a_n).
\end{aligned}\tag{4.7}$$

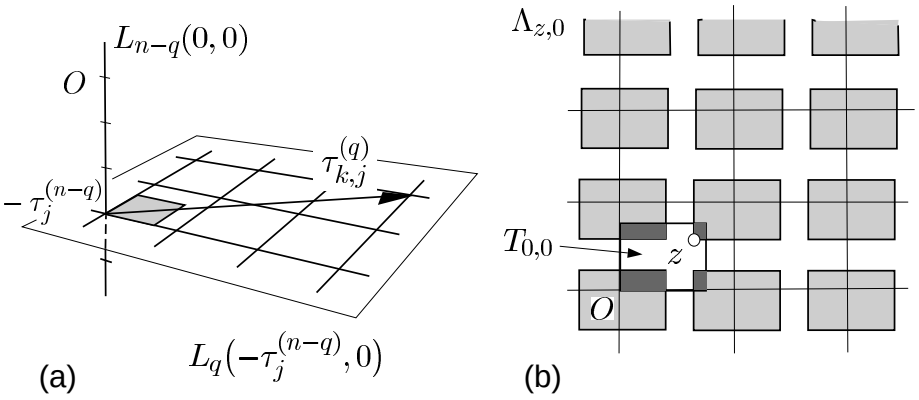

Figure 4 (a), illustration of the notation used in Subsection 4.2 to construct a test system of $q-$plates. (b), illustration of Eq. (4.11).

For the translations τ_k used to construct $\Lambda_{0,0}$ we adopt the following notation, see also Fig. 4(a),

- $\tau_j^{(n-q)}\subset L_{n-q}(0,0),\ j\in\mathbb{Z}$ are translations lying in the orthogonal complement of the linear $q-$subspace $L_q(0,0)$ (which contains $T_{0,0}$).
- $\tau_{k,j}^{(q)}\subset L_q\big(-\tau_j^{(n-q)},0\big),\ j,k\in\mathbb{Z}$ are translations lying in the linear $q-$subspace parallel to $T_{0,0}$ and shifted by the translation $-\tau_j^{(n-q)}$.

Proposition 4.2. For a FUR test system $\Lambda_{z,0}$ of $q-$plate probes constructed as above, hitting a compact set $Y \subset \mathbb{R}^n$ of dimension n with a probability element given by the second factor in the right hand side of Eq. (A.26) we have,

$$\mathbb{E}\nu_q^2(Y \cap \Lambda_{z,0}) = \frac{1}{\nu_n\big(J_{0,0}\big)} \sum_{j\in\mathbb{Z}} \sum_{k\in\mathbb{Z}} \int_{L_q\left(\tau_j^{(n-q)},0\right)} k_Y(z)\, k_{T_{0,0}}\big(z+\tau_{k,j}^{(q)}\big)\, \nu_q(\mathrm{d}z), \tag{4.8}$$

where $k_Y(x)$ is the geometric covariogram of Y defined in $\mathbb{R}^n$, whereas $k_{T_{0,0}}(x)$ is the geometric covariogram of $T_{0,0}$ defined in $\mathbb{R}^q$.

Proof. Making use of Eq. (4.1) and setting $y - x = z$ we obtain,

$$\begin{aligned} \nu_n\big(J_{0,0}\big)\, \mathbb{E}\nu_q^2(Y \cap \Lambda_{z,0}) &= \int_{T_{0,0}} \nu_q(\mathrm{d}y) \int_{\Lambda_{0,0}} k_Y(y-x)\, \nu_q(\mathrm{d}x) \\ &= \int_{\mathbb{R}^n} k_Y(z)\, \nu_q(\mathrm{d}z) \int_{\mathbb{R}^n} 1_{T_{0,0}}(y)\, 1_{\Lambda_{0,0}}(y-z)\, \nu_q(\mathrm{d}y). \end{aligned} \tag{4.9}$$

The inner integral in the last expression is zero unless z lies in the linear $q-$subspace containing $T_{0,0}$, i.e.,

$$\int_{\mathbb{R}^n} 1_{T_{0,0}}(y)\, 1_{\Lambda_{0,0}}(y-z)\, \nu_q(\mathrm{d}y) = \begin{cases} \nu_q(T_{0,0} \cap \Lambda_{z,0}), & z \in L_q\big(-\tau_j^{(n-q)},0\big),\ \forall j \in \mathbb{Z}, \\ 0, & \text{otherwise.} \end{cases} \tag{4.10}$$

Further, bearing in mind that the $q-$probes $\left\{T_{z+\tau_{k,j}^{(q)},0},\ k,j \in \mathbb{Z}\right\}$ constituting $\Lambda_{z,0}$ are disjoint for each $z \in L_q\Big(-\tau_j^{(n-q)},0\Big)$, see Fig. 4(b), and recalling the definition of the covariogram, we have,

$$\begin{aligned} \nu_q(T_{0,0} \cap \Lambda_{z,0}) &= \sum_{j\in\mathbb{Z}} \sum_{k\in\mathbb{Z}} \nu_q\Big(T_{0,0} \cap T_{z+\tau_{k,j}^{(q)},0}\Big) \\ &= \sum_{j\in\mathbb{Z}} \sum_{k\in\mathbb{Z}} k_{T_{0,0}}\big(z+\tau_{k,j}^{(q)}\big), \ \ z \in L_q\big(-\tau_j^{(n-q)},0\big),\ \forall j \in \mathbb{Z}. \end{aligned} \tag{4.11}$$

Substituting the preceding results into the right hand side of Eq. (4.9) we obtain the proposed result.

Corollary 4.2. If the test system $\Lambda_{z,t}$ of $q-$plate probes is IUR hitting Y with the probability element given by Eq. (A.26), then,

$$\mathbb{E}\nu_q^2(Y \cap \Lambda_{z,0}) = \frac{1}{\nu_n\big(J_{0,0}\big)} \sum_{j\in\mathbb{Z}} \sum_{k\in\mathbb{Z}} \int_{L_q\left(\tau_j^{(n-q)},0\right)} k_Y(\|z\|)\, k_{T_{0,0}}\big(z+\tau_{k,j}^{(q)}\big)\, \nu_q(\mathrm{d}z), \tag{4.12}$$

where $k_Y(r)$ is the isotropic covariogram of Y, whereas $k_{T_{0,0}}(x)$ is the geometric covariogram of $T_{0,0}$ defined in $\mathbb{R}^q$, namely in its containing $q-$subspace.

Proof. Start from Eq. (4.4), then follow similar steps as in the preceding proof, namely as in Eq. (4.9)-(4.11) to establish the required result.

Remark 4.1. Since $T_{0,0}$ is bounded and its translations always disjoint, there is only a finite number of nonzero terms in the double summations of Eq. (4.8), (4.12).

Remark 4.2. For a 'sparse' test system with the property that there is only one nonzero term in the double summations of Eq. (4.8), (4.12), the latter two expressions are analogous to Eq. (3.4), (3.7), respectively, valid for independent bounded $q-$plate probes.

Remark 4.3. Corollary 4.2 may not be easy to use in practice unless $q = 0, 1$, (see the examples below), because the argument of $k_{T_{0,0}}$ is not a scalar but a $q-$dimensional vector. Even in the simplest cases, however, the exact results usually have to be computed numerically.

4.3 Examples for $n = 2$

The first two examples below illustrate simple applications of Eq. (4.4), whereas the third example uses Eq. (4.12). The second example can nonetheless be regarded as a special case of the third one. In all cases the hit object is a disk $Y \subset \mathbb{R}^2$ of finite diameter d. Thus, the results do not depend on the orientation of the test system.

Test system of dimension $q = 0$: square grid of test points hitting a disk. The test system $\Lambda_{0,0}$ is a square grid of test points of side s. As fundamental tile $J_{0,0}$ we adopt the square $[0, s) \times [0, s)$ and the basic point probe $T_{0,0}$ is the origin, whereby $\Lambda_{0,0} = \{(js, ks),\ j, k \in \mathbb{Z}\}$. It is convenient to apply Eq. (4.4) directly with $y = 0$ and the inner integral is a summation, namely,

$$\begin{aligned} \mathbb{E}\nu_0^2(Y \cap \Lambda_{z,t}) &= \frac{1}{s^2} \sum_{x_i \in \Lambda_{0,0}} k_Y\big(\|x_i\|\big) \\ &= \frac{1}{s^2} \sum_{j,k \in \mathbb{Z};\, s\sqrt{j^2+k^2} \le d} k_Y\left(s\sqrt{j^2+k^2}\right), \end{aligned} \tag{4.13}$$

(Kellerer, 1986), where $k_Y(r) = k_{disk}(r, d)$, see Eq. (A.37). Since the set Y is a disk the support of the corresponding covariogram is also a disk (of diameter $2d$) and therefore we can evaluate the preceding summation using symmetry properties (Fig. 5(a)). First we compute the term at the origin (namely $k_Y(0) = \nu_2(Y)$), then four times the terms at the points $\{(js, 0),\ j \in \mathbb{N}\}$ on the horizontal half axis, then four times the terms at the points $\{(js, js),\ j \in \mathbb{N}\}$ on the diagonal of the first quadrant, and finally eight times

the terms at the grid points lying between the horizontal half axis and the diagonal of the first quadrant. Thus, Eq. (4.13) becomes,

$$s^2\,\mathbb{E}\nu_0^2(Y\cap\Lambda_{z,t}) = \frac{\pi d^2}{4} + 4\sum_{j=1}^{\lfloor d/s\rfloor} k_{disk}(js,d) + 4\sum_{j=1}^{\lfloor d/(s\sqrt{2})\rfloor} k_{disk}\Big(js\sqrt{2},d\Big) + 8\sum_{j=2}^{\lfloor\sqrt{(d/s)^2-1}\rfloor}\ \sum_{k=1}^{\inf\left\{j-1,\lfloor\sqrt{(d/s)^2-j^2}\rfloor\right\}} k_{disk}\Big(s\sqrt{j^2+k^2},d\Big), \tag{4.14}$$

where $\lfloor x\rfloor$ denotes the floor of x.

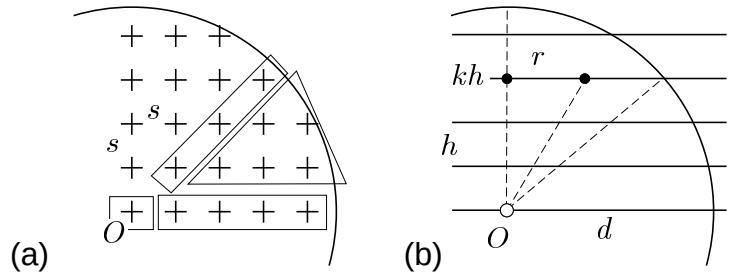

Figure 5 (a), illustration of the four different subsets of test points corresponding to the four terms in the right hand side of Eq. (4.14). (b) construction used in the derivation of Eq.(4.15) for a Cavalieri grid of test lines.

Test system of dimension $q=1$: parallel straight lines (Cavalieri grid) hitting a disk. The test system $\Lambda_{0,0}$ consists of parallel straight lines a distance h apart, (namely $\Lambda_{0,0}$ is a 'Cavalieri grid' in $\mathbb{R}^2$). As fundamental tile $J_{0,0}$ we adopt the rectangle $[0,1)\times[0,h)$ with the basic probe $T_{0,0}$ being the straight line segment $[0,1)$. Again it is simplest to apply Eq. (4.4) directly; with reference to Fig. 5(b), first we get twice the integral along the horizontal half axis, and then four times the integrals along the remaining half lines in the first quadrant. Thus,

$$\mathbb{E}\nu_1^2(Y\cap\Lambda_{z,t}) = \frac{2}{h}\int_0^d k_{disk}(r,d)\,\mathrm{d}r + \frac{4}{h}\sum_{k=1}^{\lfloor d/h\rfloor}\int_0^{\sqrt{d^2-(kh)^2}} k_{disk}\left(\sqrt{r^2+(kh)^2},d\right)\mathrm{d}r. \tag{4.15}$$

Test system of dimension $q=1$: parallel straight line segments hitting a disk. Here the fundamental tile $J_{0,0}$ of the test system $\Lambda_{0,0}$ is the rectangle $[0,s)\times[0,h)$, and the basic probe $T_{0,0}$ is the straight line segment $[0,ps)$, where $p\in(0,1)$ is fixed. Thus, $\Lambda_{0,0}$ consists of parallel straight line segments of fixed length ps. The test system may be regarded as one of $1-$plate probes, and Eq. (4.12) may be applied. First we operate on

the axis of abscissas, then on each of the parallel lines a distance h apart on the upper half plane, see Fig. 6. The result has the following expression, which is amenable to direct

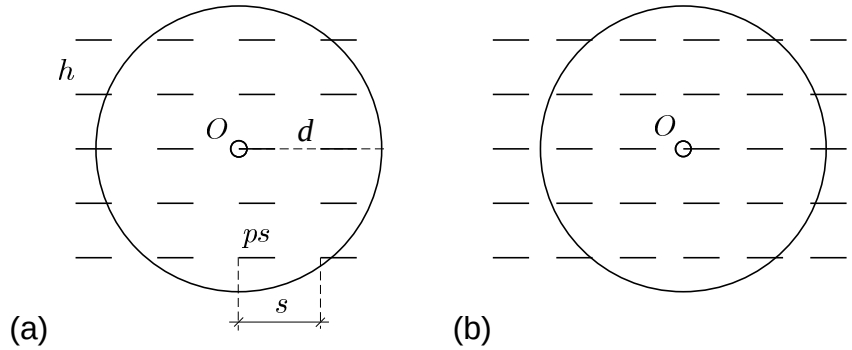

$1 - p - \text{frac}(d/s) < 0$ $\qquad$ $1 - p - \text{frac}(d/s) > 0$

Figure 6 Construction used to evaluate the second moment of the intersection between a fixed disk Y of diameter d and a uniform random test system of parallel straight line segments, see Eq. (4.16). The two disks have radius d because they correspond to the geometric covariogram of Y.

computation using for instance the command `NIntegrate[]` from MATHEMATICA®,

$$\begin{aligned}\mathbb{E}\nu_1^2(Y \cap \Lambda_{z,0}) = \frac{2}{hs} \sum_{j=-\lceil d/s \rceil + U(p,s,d)}^{\lfloor d/s \rfloor} \int_{\sup\{-d, js\}}^{\inf\{d, js+ps\}} k_{disk}(|z|, d)\, k_{seg}\big(z - js, ps\big)\, \mathrm{d}z \\ + \frac{4}{hs} \sum_{k=1}^{\lfloor d/h \rfloor} \sum_{j=-\left\lceil \sqrt{d^2-(kh)^2}/s \right\rceil + U\left(p,s,\sqrt{d^2-(kh)^2}\right)}^{\left\lfloor \sqrt{d^2-(kh)^2}/s \right\rfloor} \\ \times \int_{\sup\left\{-\sqrt{d^2-(kh)^2}, js\right\}}^{\inf\left\{\sqrt{d^2-(kh)^2}, js+ps\right\}} k_{disk}\Big(\sqrt{z^2 + (kh)^2}, d\Big)\, k_{seg}\big(z - js, ps\big)\, \mathrm{d}z,\end{aligned} \tag{4.16}$$

where $\lfloor x \rfloor, \lceil x \rceil$ denote the floor and the ceiling of x, respectively, whereas

$$U(p, s, d) = 1_{[0,1]}\big(1 - p - \text{frac}(d/s)\big), \tag{4.17}$$

and $\text{frac}(x)$ represents the fractional part of x. For instance $U(p, s, d) = 0$ for the example illustrated in Fig. 6(a), whereas $U(p, s, d) = 1$ in Fig. 6(b). In MATHEMATICA® the corresponding function is `UnitStep[]`. The first term of the right hand side of Eq. (4.16) bears a factor "2" because the range of integration of $k_{seg}(r, ps)$ on the horizontal axis is a subset of the interval $[0, ps]$, and by symmetry the result is identical for the interval $[-ps, 0]$. In addition, the second term pertains to the upper half plane only (namely $k \geq 1$), hence the factor "4".

5. VARIANCE COMPARISONS FOR BOUNDED TEST PROBES

Let $Y_k \subset \mathbb{R}^n$ denote a bounded $k-$dimensional set , $k \leq n$, with $\nu_k(Y_k) > 0$, which is the quantity to be estimated. To this end consider two alternative bounded probes, namely a $q-$dimensional probe $T_{0,0}^{(q)}$ and a $r-$dimensional subprobe $T_{0,0}^{(r)}$ such that $T_{0,0}^{(r)} \subset T_{0,0}^{(q)}$ and $n-k \leq r < q \leq n$. Our purpose is to compare the variances of the corresponding estimators of $\nu_k(Y_k)$ obtained with either probe.

Suppose that the $q-$probe is IUR hitting Y_k with the probability element given by Eq. (A.18). Then by virtue of Eq. (A.21) the estimator

$$\widehat{\nu}_k(Y_k) = c_{k,q,n} \cdot \nu_{k+q-n}\big(Y \cap T_{x,t}^{(q)}\big), \tag{5.1}$$

is a one stage unbiased estimator of $\nu_k(Y_k)$, where $c_{k,q,n}$ is a constant of dimension $n-q$. In the following two subsections we distinguish between two different sampling regimes, namely lower dimensional subsampling, and direct lower dimensional sampling, respectively.

5.1 **Probe sampling with independent subsampling**

Here we consider the classical situation in which the probe $T_{0,0}^{(q)}$ and the subprobe $T_{0,0}^{(r)}$ are used to estimate $\nu_k(Y_k)$ by a two stage sampling procedure (Cochran, 1977) in which the subprobe is randomized for each position of the primary probe (Cruz-Orive, 1980). More precisely, for each pair (x,t) the subprobe $T_{0,0}^{(r)}$ is IUR hitting the first stage intersection $Y_k \cap T_{x,t}^{(q)}$ whereby we obtain an unbiased estimator $\widehat{\nu}_{k+q-n}\big(Y \cap T_{x,t}^{(q)}\big)$ of $\nu_{k+q-n}\big(Y \cap T_{x,t}^{(q)}\big)$. Therefore,

$$\widetilde{\nu}_k(Y_k) = c_{k,q,n} \cdot \widehat{\nu}_{k+q-n}\big(Y \cap T_{x,t}^{(q)}\big), \tag{5.2}$$

is a two stage unbiased estimator of $\nu_k(Y_k)$. Under the preceding conditions the following version of the classical Rao-Blackwell theorem holds (Baddeley & Cruz-Orive, 1995).

Theorem 5.1, (stereological Rao-Blackwell).

$$\mathrm{Var}\big(\widetilde{\nu}_k(Y_k)\big) \geq \mathrm{Var}\big(\widehat{\nu}_k(Y_k)\big). \tag{5.3}$$

5.2 **Direct lower dimensional sampling: Variance paradoxes of Jensen–Gundersen type**

Suppose that the subprobe $T_{0,0}^{(r)}$ is IUR hitting the set Y_k directly, namely $T_{0,0}^{(r)}$ is not used to estimate a first stage statistic such as $\nu_{k+q-n}\big(Y \cap T_{x,t}^{(q)}\big)$, but to estimate $\nu_k(Y_k)$ directly. In other words, when the primary probe $T_{0,0}^{(q)}$ is IUR hitting Y_k, the subprobe $T_{0,0}^{(r)}$ is not randomized, but instead it remains rigidly attached to $T_{0,0}^{(q)}$ and we observe

$Y_k \cap T_{x,t}^{(r)}$ directly. Under such circumstances we do not obtain a second stage unbiased estimator $\widehat{\nu}_{k+q-n}\big(Y \cap T_{x,t}^{(q)}\big)$ of $\nu_{k+q-n}\big(Y \cap T_{x,t}^{(q)}\big)$, and therefore the inequality (5.3) does not need to apply even if $r < q$.

The preceding fact originated a lively controversy for years after Jensen & Gundersen (1982) described an example in which $Y_2 \subset \mathbb{R}^2$ was a disk of diameter $d = 4$ and the target parameter was the boundary length to area ratio $R := \nu_1(\partial Y_2)/\nu_2(Y_2)$. To estimate R two alternative probes were used: $T_{0,0}^{(2)}$ was the unit square whereas $T_{0,0}^{(0)}$ was the union of the four vertices of the unit square. For IUR $T_{0,0}^{(2)}$ hitting Y_2 they first considered the direct estimator of R namely,

$$\widehat{R} = \frac{\nu_1\big(\partial Y_2 \cap T_{x,t}^{(2)}\big)}{\nu_2\big(Y_2 \cap T_{x,t}^{(2)}\big)}, \tag{5.4}$$

that is, the ratio of the observable circle length to disk area in the square probe. On the other hand they constructed the alternative estimator

$$\widetilde{R} = \frac{\pi}{2} \cdot \frac{\nu_0\big(\partial Y_2 \cap \partial T_{x,t}^{(2)}\big)}{\nu_0\big(Y_2 \cap T_{x,t}^{(0)}\big)}, \tag{5.5}$$

namely $\pi/2$ times the ratio of the number of intersections between disk and square boundaries to the number of vertices inside the disk. For each estimator the ratio of the expectations of numerator and denominator is equal to the target ratio R but, intuitively $\widehat{R}$ would seem to be more precise than $\widetilde{R}$ because it incorporates more information. Yet, the aforementioned authors discovered that, at least for $d = 4$, $\mathrm{Var}\big(\widetilde{R}\big) < \mathrm{Var}\big(\widehat{R}\big)$. A similar example was reworked in Baddeley & Cruz-Orive (1995) for variable d.

A key question is: which precise shape conditions should a lower dimensional subprobe $T_{0,0}^{(r)}$ enjoy to be more precise than its containing probe $T_{0,0}^{(q)}$? This question can hitherto not be answered in its full generality, but as shown below some additional light may be thrown into it with the aid of new examples.

5.3 **Examples: fixed disk probed by a straight line segment, and by a pair of points**

The target parameter is the area $\nu_2(Y)$ of a disk $Y \subset \mathbb{R}^2$ of diameter d. We want to compare the estimation variances for three alternative sampling probes, namely a straight line segment $T_{0,0}^{(1)}$ of length l, the union of the two end points $T_{0,0}^{(0)}$ of $T_{0,0}^{(1)}$, see Fig. 2(b), and finally a straight line segment $\widetilde{T}_{0,0}^{(1)}$ of length $2l$. To facilitate the comparisons we assume that each probe is IUR hitting a disk X of area A such that $Y \oplus \big(-\widetilde{T}_{0,t}\big) \subset X$, $\forall t \in G_{2[0]}$. Thus the common probability element is,

$$\mathbb{P}(\mathrm{d}z, \mathrm{d}t) = (2\pi A)^{-1} \nu_2(\mathrm{d}x)\, \mathrm{d}t,\ x \in X,\ t \in \mathbb{S}. \tag{5.6}$$

For $T_{0,0}^{(1)}$ the unbiased estimator of $\nu_2(Y)$ is,

$$\widehat{\nu}_2\big(Y,T^{(1)}\big) = \frac{A}{l}\,\nu_1\big(Y\cap T_{x,t}^{(1)}\big). \tag{5.7}$$

For $d < l < \infty$ the second Eq. (3.11) leads to

$$\mathrm{Var}\big\{\widehat{\nu}_2\big(Y,T^{(1)}\big)\big\} = \frac{A}{l^2}\left(\frac{2}{3}ld^3 - \frac{\pi}{16}d^4\right) - \nu_2^2(Y). \tag{5.8}$$

The corresponding results for $T_{0,0}^{(0)}$ are,

$$\widehat{\nu}_2\big(Y,T^{(0)}\big) = \frac{A}{2}\,\nu_0\big(Y\cap T_{x,t}^{(0)}\big), \tag{5.9}$$

and, making use of Eq. (3.3),

$$\begin{aligned}\mathrm{Var}\big\{\widehat{\nu}_2\big(Y,T^{(0)}\big)\big\} &= \frac{A}{4}\big(2k_Y(0)+2k_Y(l)\big) - \nu_2^2(Y)\\ &= \frac{A}{8}\cdot\pi d^2 - \nu_2^2(Y),\end{aligned} \tag{5.10}$$

respectively. In the preceding result we have used the identities $k_Y(0) = \nu_2(Y)$ and $k_Y(l) = 0$, $l \geq d$. It is easy to verify that the inequality

$$\mathrm{Var}\big\{\widehat{\nu}_2\big(Y,T^{(0)}\big)\big\} \leq \mathrm{Var}\big\{\widehat{\nu}_2\big(Y,T^{(1)}\big)\big\} \tag{5.11}$$

holds for $0 < l < 1.318\,d$, (Fig. 7).

The preceding result looks paradoxical at first sight because $T_{0,0}^{(0)}$ consists of the two endpoints of $T_{0,0}^{(1)}$ only. However, for each position of $T_{x,t}^{(1)}$ hitting Y, the subprobe $T_{x,t}^{(0)}$ cannot supply an unbiased estimator of $Y\cap T_{z,t}^{(1)}$, and therefore Theorem 5.1 does not need to apply. Note also that, while $Y\cap T_{z,t}^{(1)}$ contains indeed more information than $Y\cap T_{z,t}^{(0)}$, the extra information turns out to be not only redundant but even detrimental for the particular task of estimating $\nu_2(Y)$.

To stress the foregoing ideas consider now the estimation of $\nu_2(Y)$ in two stages. The first stage probe is the straight line segment $\widetilde{T}_{0,0}^{(1)} := [0, 2l)$ of length $2l$ and the first stage estimator is,

$$\widehat{\nu}_2\big(Y,\widetilde{T}^{(1)}\big) = \frac{A}{2l}\,\nu_1\big(Y\cap \widetilde{T}_{x,t}^{(1)}\big). \tag{5.12}$$

with the density (5.6). The second stage probe is a pair of points $T_{z,0,0}^{(0)} := \{z, z+l\}$ a fixed distance l apart, like $T_{0,0}^{(0)}$; however we assume that $T_{z,0,0}^{(0)} \subset \widetilde{T}_{0,0}^{(1)}$ and z is

uniform random in $[0, l)$, so that $T^{(0)}_{z,0,0}$ is effectively a uniform random point grid in $\widetilde{T}^{(1)}_{0,0}$. Consequently,

$$\mathbb{E}\,\nu_0\big(Y \cap \widetilde{T}^{(1)}_{x,t} \cap \widetilde{T}^{(0)}_{z,x,t}\big) = l^{-1}\nu_1\big(Y \cap \widetilde{T}^{(1)}_{x,t}\big). \tag{5.13}$$

Recalling Eq. (5.12) the two stage unbiased estimator of $\nu_2(Y)$ may be written

$$\widetilde{\nu}_2\big(Y, \widetilde{T}^{(0)}\big) = \frac{A}{2}\,\nu_0\big(Y \cap \widetilde{T}^{(1)}_{x,t} \cap \widetilde{T}^{(0)}_{z,x,t}\big). \tag{5.14}$$

Since the preceding estimator is connected with $\widehat{\nu}_2\big(Y, \widetilde{T}^{(1)}\big)$ via Eq. (5.13), now Theorem 5.1 applies and therefore it can be anticipated that

$$\mathrm{Var}\big\{\widetilde{\nu}_2\big(Y, \widetilde{T}^{(0)}\big)\big\} \geq \mathrm{Var}\big\{\widehat{\nu}_2\big(Y, \widetilde{T}^{(1)}\big)\big\}. \tag{5.15}$$

It is noteworthy that the estimator $\widetilde{\nu}_2\big(Y, \widetilde{T}^{(0)}\big)$ has the same distribution as $\widehat{\nu}_2\big(Y, T^{(0)}\big)$

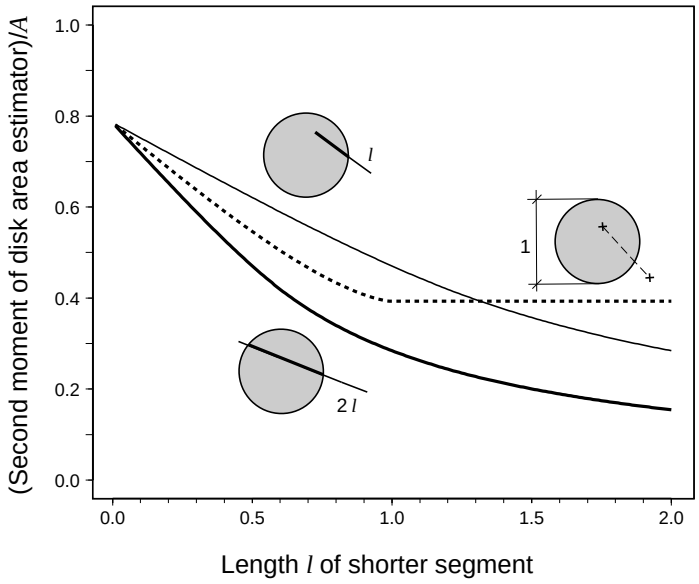

Figure 7 A simple variance 'paradox' of Jensen-Gundersen type. The system of two test points a distance l apart can entirely sweep a test segment of length $2l$ always remaining within the segment, but this is not the case for a test segment of length l. As a consequence the longer test segment is always the more efficient, but the segment of length l is not necessarily more efficient than the two point test system. See Subsection 5.3 and Fig. 2.

because a uniform random grid of points within a line segment which moves with the kinematic measure in $\mathbb{R}^2$ is a grid of points moving with the kinematic measure in $\mathbb{R}^2$. Thus the performance of the two end points of a segment of length l is improved by that of a segment of length $2l$, but not necessarily by one of length l, see Fig. 7. One may think that, in fact, point counting with the two endpoints of a IUR line segment uses somehow information outside the segment itself, because the two points could be used to estimate the length of a line segment twice as long.

Remark 5.1. Consider the following three sampling probes to estimate the area $\nu_2(Y)$ of a disk $Y \subset \mathbb{R}^2$ of diameter d, namely: the set $T_{0,0}^{(0)}$ of the four vertices of a square of side s, the actual square $T_{0,0}^{(2)}$ of side s, and another square $\widetilde{T}_{0,0}^{(2)}$ of side $2s$. By analogy with the preceding results we find that the estimator of $\nu_2(Y)$ based on $T_{0,0}^{(0)}$ is more efficient than that based on $T_{0,0}^{(2)}$ for $d/s > 0.710...$, (Baddeley & Cruz-Orive, 1995), but always less efficient than that based on $\widetilde{T}_{0,0}^{(2)}$.

5.4 **Examples: test probes of dimension** 0, 1, 2 **hitting a fixed square**

Here the target parameter is the area $\nu_2(Y)$ of a square $Y \subset \mathbb{R}^2$ of side length d. We consider, in turn, four alternative sampling probes namely: the set $T_{0,0}^{(0)}$ of the four vertices of a square of side length s, the boundary $T_{0,0}^{(1)}$ of the corresponding square, the circumdisk $T_{0,0}^{(2)}$ of the square, (that is, a disk of diameter $l := s\sqrt{2}$), and finally the boundary $\widetilde{T}_{0,0}^{(1)}$

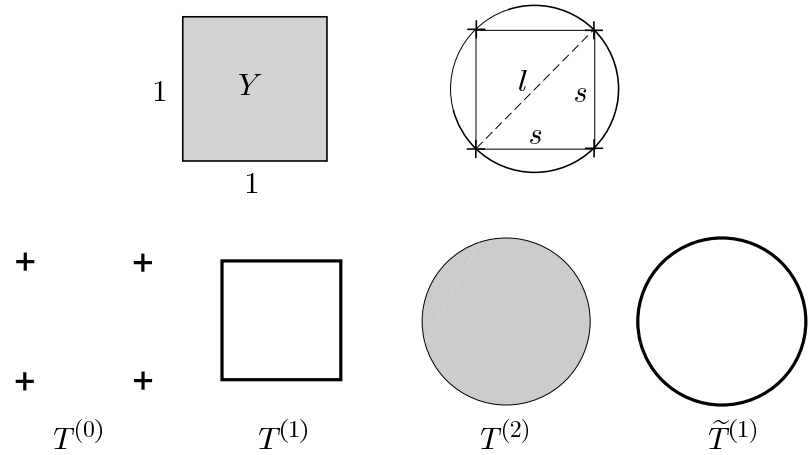

Figure 8 Lower row: the four probes used in Subsection 5.4 to construct new variance paradoxes of Jensen-Gundersen type. The square of side length $d = 1$ (upper row) represents the fixed figure to be sampled. The corresponding results are plotted in Fig. 9.

of this disk, see Fig. 8. Thus $T_{0,0}^{(0)} \subset T_{0,0}^{(1)} \subset T_{0,0}^{(2)}$ and also $T_{0,0}^{(0)} \subset \widetilde{T}_{0,0}^{(1)} \subset T_{0,0}^{(2)}$. The four probes are IUR hitting Y with a common probability element given by Eq. (5.6), where X is a disk of area A such that $Y \oplus \breve{T}_{0,0}^{(2)} \subset X$. The corresponding unbiased estimators are,

$$\begin{aligned}
\widehat{\nu}_2\big(Y, T^{(0)}\big) &= \frac{A}{4}\,\nu_0\big(Y \cap T_{x,t}^{(0)}\big),\\
\widehat{\nu}_2\big(Y, T^{(1)}\big) &= \frac{\sqrt{2}A}{4l}\,\nu_1\big(Y \cap T_{x,t}^{(1)}\big),\\
\widetilde{\nu}_2\big(Y, \widetilde{T}^{(1)}\big) &= \frac{A}{\pi l}\,\nu_1\big(Y \cap \widetilde{T}_{x,t}^{(1)}\big),\\
\widehat{\nu}_2\big(Y, T^{(2)}\big) &= \frac{4A}{\pi l^2}\,\nu_2\big(Y \cap T_{x,t}^{(2)}\big).
\end{aligned} \tag{5.16}$$

respectively. The second moments of the preceding estimators are plotted in Fig. 9. The second moment $\mathbb{E}\widehat{\nu}_2^2\big(Y, T^{(0)}\big)$ was computed via Eq. (C.2), whereas $\mathbb{E}\widehat{\nu}_2^2\big(Y, T^{(1)}\big)$ was computed from Eq. (C.1), $\mathbb{E}\widehat{\nu}_2^2\big(Y, \widetilde{T}^{(1)}\big)$ from Eq. (3.15), and $\mathbb{E}\widehat{\nu}_2^2\big(Y, T^{(2)}\big)$ from Eq. (3.10).

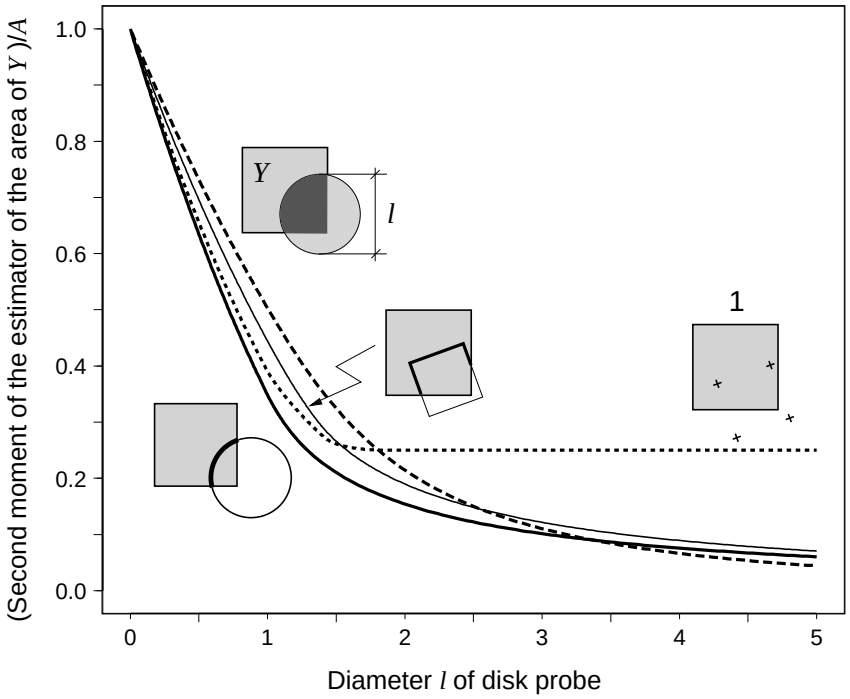

Figure 9 Efficiency comparisons among the four bounded test probes represented in Fig. 8. See discussion in Subsection 5.4.

From Fig. 9 the following conclusions may be drawn:

(1). The point counting estimator $\widehat{\nu}_2\big(Y, T^{(0)}\big)$ is not necessarily less efficient than either the length measurement estimator $\widehat{\nu}_2\big(Y, T^{(1)}\big)$ with the square boundary, nor the area measurement estimator $\widehat{\nu}_2\big(Y, T^{(2)}\big)$. This is because Theorem 5.1 is not applicable in either case.

(2). The length measurement estimator with the circle boundary, namely $\widehat{\nu}_2\big(Y, \widetilde{T}^{(1)}\big)$, is not necessarily less efficient than the area measurement estimator $\widehat{\nu}_2\big(Y, T^{(2)}\big)$, and it is always more efficient than the length measurement estimator with the square boundary, $\widehat{\nu}_2\big(Y, T^{(1)}\big)$, and also than the point counting estimator $\widehat{\nu}_2\big(Y, T^{(0)}\big)$. The first fact holds because Theorem 5.1 is not applicable, and the third statement is again a consequence of Theorem 5.1. To see this, suppose that the four point square grid $T_{x,t}^{(0)}$ of side s is contained in the circle $\widetilde{T}_{x,0}^{(1)}$ of diameter $l = s\sqrt{2}$, where t represents the arc distance of one of the points of the grid from a fixed point in $\widetilde{T}_{x,0}^{(1)}$. Imagine that the point grid is rotated uniformly at random within $\widetilde{T}_{x,0}^{(1)}$, namely that t is a uniform random variable in the interval $(0, \pi l/4)$. Then clearly for each pair (x, t) the factor $\nu_1\big(Y \cap \widetilde{T}_{x,t}^{(1)}\big)$ in the right hand side of the third Eq. (5.16) may be estimated without bias with the point grid. Replacing $\nu_1\big(Y \cap \widetilde{T}_{x,t}^{(1)}\big)$ with the

corresponding estimator in the right hand side of the third Eq. (5.16) we obtain a two stage unbiased estimator of $\nu_2(Y)$ with identical distribution as $\widehat{\nu}_2\big(Y, T^{(0)}\big)$, because a uniform grid of points within a circle which moves with the kinematic measure in $\mathbb{R}^2$ is a grid of points moving with the kinematic measure in $\mathbb{R}^2$. Therefore, by Theorem 5.1 $\widehat{\nu}_2\big(Y, \widetilde{T}^{(1)}\big)$ is always more efficient than $\widehat{\nu}_2\big(Y, T^{(0)}\big)$. Indeed, the same result holds if the four point grid is replaced with a uniform grid of k equispaced test points in the circle: the test grid will always be less efficient than the test circle.

6. VARIANCE COMPARISONS FOR TEST SYSTEMS

6.1 **Extension from bounded test probes to test systems**

The results from the preceding section trivially extend to 'dilute' test systems of $q-$probes, namely test systems for which the maximum number of $q-$probes hitting the target set $Y_k \subset \mathbb{R}^n$ is 1. To extend the mentioned results to test systems, however, diluteness is not a necessary property — in fact, the stereological Rao-Blackwell theorem is concerned with unbiased sampling and subsampling only, with no assumptions whatsoever about probe shape.

In the next subsection we describe an example in which Theorem 5.1 holds, and a second example in which the theorem does not hold. The necessary tools are borrowed from Section 4.

6.2 **Jensen–Gundersen type paradoxes for test systems**

The target parameter is again the area $\nu_2(Y)$ of a disk $Y \subset \mathbb{R}^2$ of diameter d. First we compare the performance of the following two test systems, see Fig. 10.

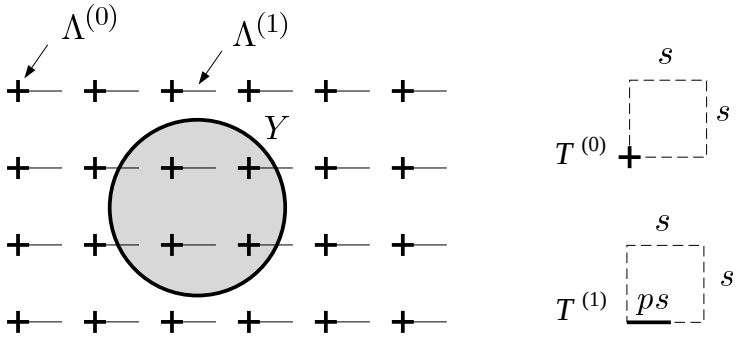

Figure 10 Two systems $\Lambda^{(0)}$ and $\Lambda^{(1)}$ of test points and test segments respectively, (here represented simultaneously), whose relative efficiency is studied in Subsection 6.2. The test point system $\Lambda^{(0)}$ can sweep the test segment system $\Lambda^{(1)}$ entirely, always remaining within $\Lambda^{(1)}$. For this reason $\Lambda^{(1)}$ is always more efficient than $\Lambda^{(0)}$. See also Fig. 11.

- A square grid $\Lambda^{(0)}_{0,0}$ of test points of side s, namely $J_{0,0} = [0, s) \times [0, s)$ and $T^{(0)}_{0,0} = (0, 0)$.
- A system $\Lambda^{(1)}_{0,0}$ of parallel test segments of length ps, $p \in (0, 1]$, namely $J_{0,0} = [0, s) \times [0, s)$ and $T^{(1)}_{0,0} = [0, ps)$.

When the test systems are IUR hitting Y, the corresponding unbiased estimators are

$$\begin{aligned}\widehat{\nu}_2\big(Y,\Lambda^{(0)}\big) &= s^2\nu_0\big(Y\cap\Lambda^{(0)}_{x,t}\big),\\ \widehat{\nu}_2\big(Y,\Lambda^{(1)}\big) &= \frac{s}{p}\,\nu_1\big(Y\cap\Lambda^{(1)}_{x,t}\big),\end{aligned} \tag{6.1}$$

respectively. Direct computations from Eq. (4.14), from (4.16) for $p = 0.1, 0.5, 0.75$, and from Eq. (4.15), (which is equivalent to $p = 1$), see Fig. 11, suggest that

$$\mathrm{Var}\big\{\widehat{\nu}_2\big(Y,\Lambda^{(0)}\big)\big\} \geq \mathrm{Var}\big\{\widehat{\nu}_2\big(Y,\Lambda^{(1)}\big)\big\}. \tag{6.2}$$

The preceding inequality is in fact a consequence of Theorem 5.1. To establish this

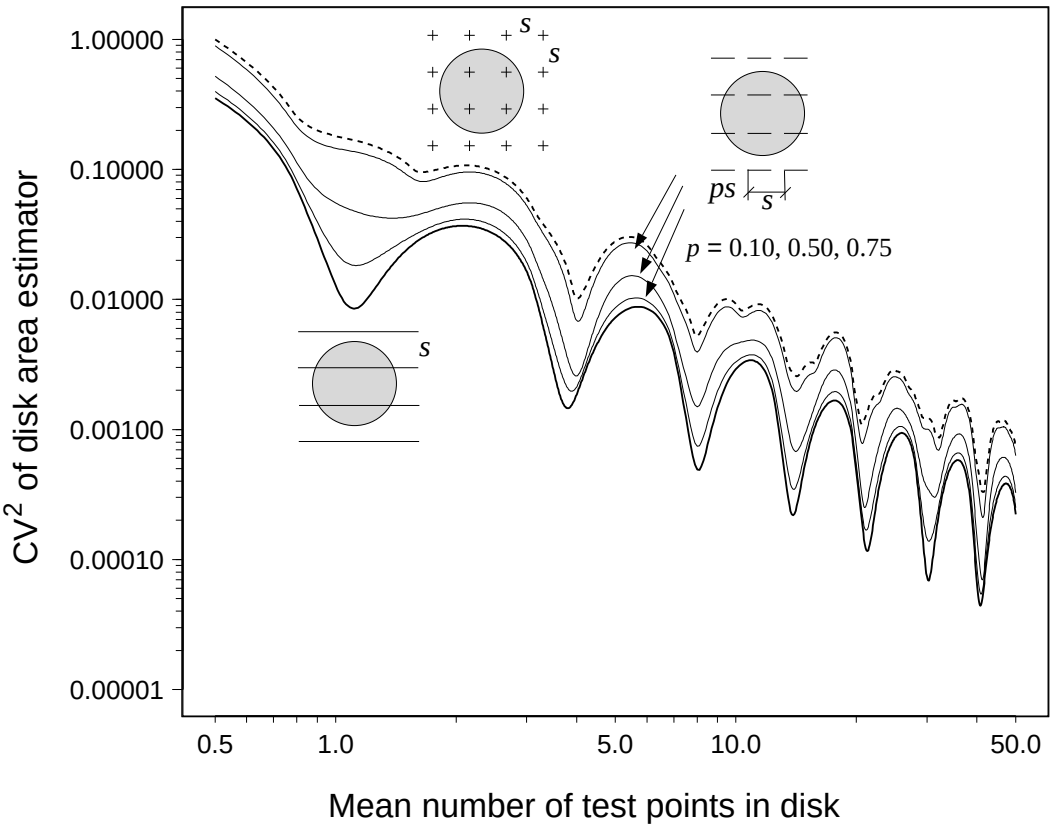

Figure 11 Efficiency comparisons among disk area estimators obtained from test point counts and from the total length of the intercepts determined in the disk by test systems of segments of increasing length ps. There appears to be a continuity in the behaviour of the square coefficient of variation from $p = 0$ (test points) and $p = 1$ (Cavalieri grid of parallel test lines). As explained in the text, Subsection 5.4, and in the legend to Fig. 10, here the stereological Rao-Blackwell theorem applies throughout.

regard the grid of segments $\Lambda^{(1)}_{0,0}$ as a first stage probe, and consequently $\widehat{\nu}_2\big(Y,\Lambda^{(1)}\big)$, see Eq. (6.1), as a first stage estimator. Next, for each pair (x,t) adopt the point grid $\Lambda^{(0)}_{z,x,t} \subset \Lambda^{(1)}_{x,t}$, (congruent with $\Lambda^{(0)}_{0,0}$), as a subprobe of $\Lambda^{(1)}_{x,t}$, where z represents the distance

of a test point of $\Lambda^{(0)}_{z,x,t}$ from the left endpoint of a test segment of $\Lambda^{(1)}_{x,t}$. If z is a uniform random variable in the interval $(0, ps)$, then $\Lambda^{(0)}_{z,x,t}$ is a uniform random second stage probe hitting $\Lambda^{(1)}_{x,t}$ and therefore

$$\mathbb{E}\,\nu_0\big(Y \cap \Lambda^{(1)}_{x,t} \cap \Lambda^{(0)}_{z,x,t}\big) = (ps)^{-1}\nu_1\big(Y \cap \Lambda^{(1)}_{x,t}\big), \tag{6.3}$$

which combined with the second Eq. (6.1) yields the two stage unbiased estimator

$$\widetilde{\nu}_2\big(Y \cap \Lambda^{(0)}_z\big) = s^2\ \nu_0\big(Y \cap \Lambda^{(1)}_{x,t} \cap \Lambda^{(0)}_{z,x,t}\big). \tag{6.4}$$

Now Theorem 5.1 applies, and therefore,

$$\mathrm{Var}\big\{\widetilde{\nu}_2\big(Y, \Lambda^{(0)}_z\big)\big\} \geq \mathrm{Var}\big\{\widehat{\nu}_2\big(Y, \Lambda^{(1)}\big)\big\}. \tag{6.5}$$

But $\widetilde{\nu}_2\big(Y, \Lambda^{(0)}_z\big)$ and $\widehat{\nu}_2\big(Y, \Lambda^{(0)}\big)$ have identical distributions because a uniform random grid of points $\Lambda^{(0)}_{z,x,t}$ within a line segment grid $\Lambda^{(1)}_{x,t}$ which moves with the kinematic measure in $\mathbb{R}^2$ is a grid of points moving with the kinematic measure in $\mathbb{R}^2$. Therefore Eq. (6.5) may be written as Eq. (6.2).

Now we describe an example in which Theorem 5.1 does not apply. The target parameter is the same as above, and we want to compare the performance of the following two test systems, see Fig.12.

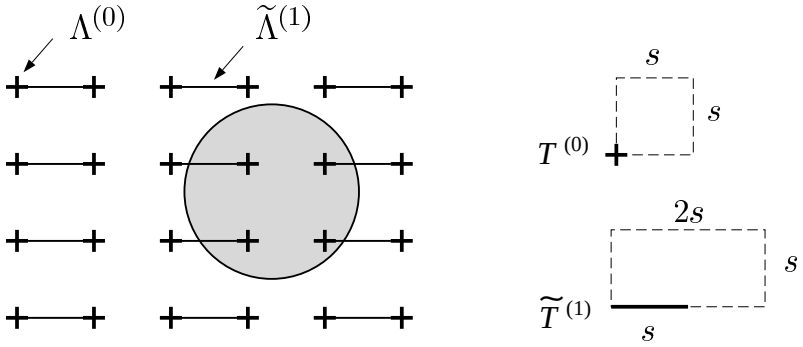

Figure 12 Contrary to the case illustrated in Fig. 10, here the test point system $\Lambda^{(0)}$ cannot sweep the test segment system $\widetilde{\Lambda}^{(1)}$ always remaining within $\widetilde{\Lambda}^{(1)}$. Therefore the stereological Rao-Blackwell theorem does not apply in this case, and $\widetilde{\Lambda}^{(1)}$ is not necessarily more efficient than $\Lambda^{(0)}$. See Subsection 6.2 and Fig. 13.

- The square grid $\Lambda^{(0)}_{0,0}$ of test points of side s considered above.
- A system $\widetilde{\Lambda}^{(1)}_{0,0}$ of parallel test segments of length s, with fundamental tile $J_{0,0} = [0, 2s) \times [0, s)$ and $\widetilde{T}^{(1)}_{0,0} = [0, s)$.

When the test systems are IUR hitting Y, the unbiased estimator corresponding to $\Lambda^{(0)}_{0,0}$ is $\widehat{\nu}_2\big(Y,\Lambda^{(0)}\big)$, see the first Eq. (6.1), whereas the one corresponding to $\widetilde{\Lambda}^{(1)}_{0,0}$ is

$$\widetilde{\nu}_2\big(Y,\widetilde{\Lambda}^{(1)}\big) = 2s\,\nu_1\big(Y\cap\widetilde{\Lambda}^{(1)}_{x,t}\big). \tag{6.6}$$

Now, however, $\Lambda^{(0)}_{0,0}$ cannot be adopted as a subprobe moving within $\widetilde{\Lambda}^{(1)}_{0,0}$, and therefore the conditions underlying Theorem 5.1 cannot be implemented. As a consequence the inequality

$$\mathrm{Var}\big\{\widehat{\nu}_2\big(Y,\Lambda^{(0)}\big)\big\} \le \mathrm{Var}\big\{\widetilde{\nu}_2\big(Y,\widetilde{\Lambda}^{(1)}\big)\big\} \tag{6.7}$$

may hold for at least some values of the ratio d/s. This is indeed confirmed by numerical computation from Eq. (4.16), see Fig. 13.

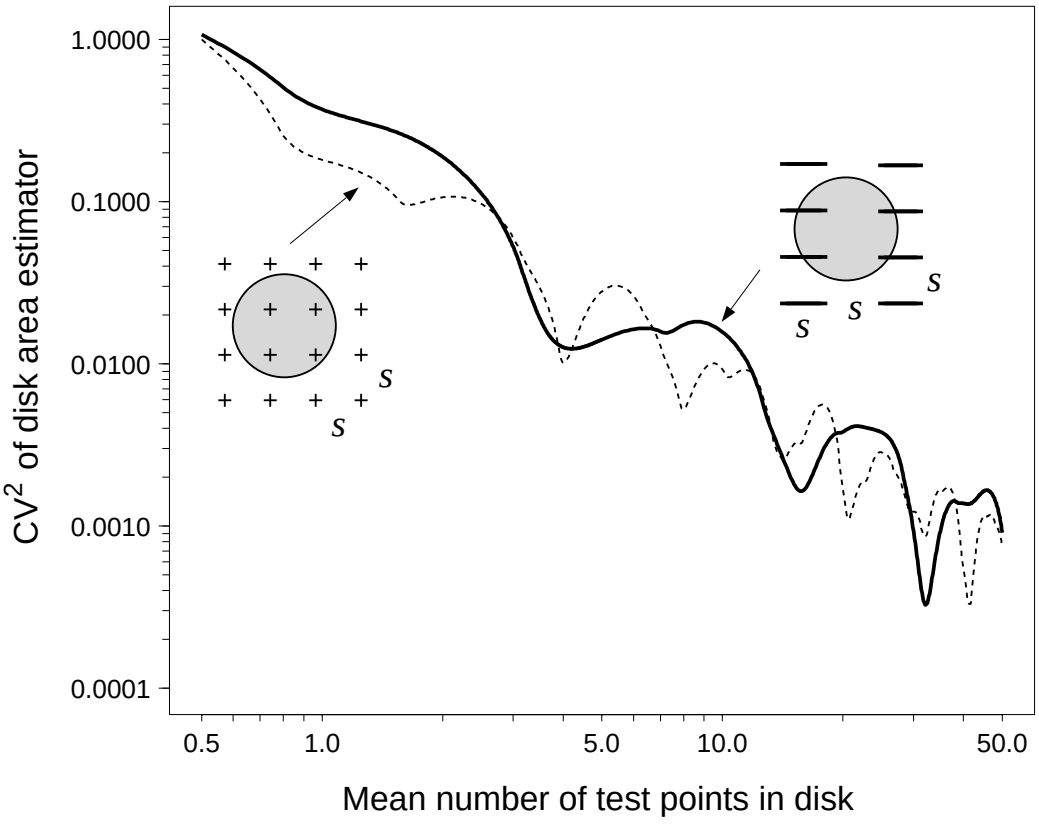

Figure 13 Results anticipated in the legend to Fig. 12.

7. POISSON PROCESSES OF $q-$FLATS AND OF BOUNDED $q-$PROBES

7.1 **Preliminaries**

The results given in Sections 2 and 3 are extensible to Poisson processes of $q-$flats and of $q-$dimensional bounded subsets (called $q-$subsets here, for short) respectively. The basic definitions are given in Appendix B; in the present case the family $\mathbb{M}_q$ of subsets introduced in Section B.1 is the family of $q-$objects (such as $q-$flats $L_q(z_k,t_k)$,

$q-$subsets $T^{(q)}_{x_k,t_k}$, etc.) constituting the Poisson process Φ with realizations in $\mathbb{R}^n$. For simplicity the kth $q-$object will be denoted by $T^{(q)}_k$, $k \in \mathbb{N}$. Thus, either type of Poisson process may be represented as $\Phi := \bigcup_{k\in\mathbb{N}} T^{(q)}_k$.

A basic difference between the design based approach adopted in the foregoing sections and the model based approach adopted here is that the roles of the probe and the compact set Y are exchanged. Thus, copies of the formerly known probes now constitute the $q-$objects constituting an unknown random set Φ, with realizations in $\mathbb{R}^n$, whose geometric parameters have to be estimated, whereas the unknown set Y is replaced with a known, compact $n-$dimensional sampling window W. In this context an estimator f is a function of the $q-$objects which intersect W only. More precisely,

$$f : \mathbb{M}_q \to \mathbb{R}^+ : \ f(\varphi) = f\big(\{T^{(q)}_k \subset \varphi : T^{(q)}_k \cap W \neq \emptyset, k \in \mathbb{N}\}\big). \tag{7.1}$$

A fundamental property of a stationary (or homogeneous) Poisson process Φ is its intensity λ_Φ, see Eq. (B.3). A Poisson $q-$flat process of intensity λ_Φ in $\mathbb{R}^n$ is equivalent to a marked Poisson point process of intensity λ_Φ in $\mathbb{R}^{n-q}$ with independent marks in $G_{q,n-q}$. For instance, suppose that Φ is a homogeneous Poisson process of straight lines in $\mathbb{R}^2$ (Miles, 1964), and $W \subset \mathbb{R}^2$ a fixed convex window. Then the mean number N of Poisson lines hitting W is $\mathbb{E}N = \lambda_\Phi\, \nu_1(\partial W)/\pi$. Further, the mean length of a Poisson chord in W is the mean chord length of a IUR test line hitting W, namely $\pi\nu_2(W)/\nu_1(\partial W)$; hence the mean total chord length in W is $\mathbb{E}\nu_1(\Phi \cap W) = \lambda_\Phi \nu_2(W)$, which is the original definition of λ_Φ. On the other hand, a stationary Poisson $q-$subset process is a germ-grain model (Stoyan *et al*., 1995) in which the germs are the $q-$subsets $T^{(q)}_k$ and the germs $\{x_k\}$ constitute a stationary Poisson point process of intensity $\lambda^{(0)}_\Phi$. To simplify the exposition we assume that the $T^{(q)}_k$ are all congruent. As indicated in Eq. (B.7), for $q < n$ we have,

$$\lambda_\Phi = \lambda^{(0)}_\Phi \nu_q\big(T^{(q)}_1\big). \tag{7.2}$$

For a stationary Poisson process Φ of $q-$objects in $\mathbb{R}^n$ the random number of $q-$objects hitting a convex window W, namely

$$N := \ \#\big\{k \in \mathbb{N} : \ W \cap T^{(q)}_k \neq \emptyset\big\}, \tag{7.3}$$

has Poisson distribution with mean

$$\lambda := \mathbb{E}N = \begin{cases} \lambda_\Phi\, \mathbb{E}_t \nu_{n-q}(W'_t) & \text{if the process is of } q-\text{flats,} \\ \\ \lambda_\Phi\, \nu_q^{-1}\big(T^{(q)}_1\big)\, \mathbb{E}_t \nu_n\big(W_t \oplus \breve{T}^{(q)}_1\big) & \text{if the process is of } q-\text{subsets.} \end{cases} \tag{7.4}$$

where $W_t \subset \mathbb{R}^n$ denotes the window with orientation $t \in G_{n[0]}$.

7.2 **Second moment formulae**

Suppose that the estimator f, defined by Eq. (7.1) for a given convex window W, is additive, namely it satisfies the identity $f\big(\bigcup_{k\in\mathbb{N}} T_k^{(q)}\big) = \sum_{k\in\mathbb{N}} f\big(T_k^{(q)}\big)$, and recall Eq. (7.3), (7.4).

Proposition 7.1.

$$\mathbb{E}f^2(\Phi) = \lambda\,\mathbb{E}f^2\big(T_1^{(q)}\big) + \lambda^2\big(\mathbb{E}f\big(T_1^{(q)}\big)\big)^2. \tag{7.5}$$

Proof. Recalling the basic properties of the Poisson process listed in Section B.2 and setting $p(k;\lambda) = \lambda^k \exp(-\lambda)/k!$, $k = 0, 1, ...$, the probability function of the Poisson distribution of mean λ, we have,

$$\begin{aligned}
\mathbb{E}f^2(\Phi) &= \mathbb{E}\big\{\mathbb{E}\big(f^2(\Phi)|N\big)\big\} \\
&= \sum_{k=0}^{\infty} p(k;\lambda)\,\mathbb{E}\big(f^2(\Phi)|N=k\big) \\
&= \sum_{k=0}^{\infty} p(k;\lambda)\,\mathbb{E}\bigg(\sum_{j=1}^{k} f\big(T_k^{(q)}\big)\bigg)^2 \\
&= \mathbb{E}f^2\big(T_1^{(q)}\big)\sum_{k=0}^{\infty} kp(k;\lambda) + \Big(\mathbb{E}f\big(T_1^{(q)}\big)\Big)^2 \sum_{k=0}^{\infty} k(k-1)p(k;\lambda),
\end{aligned} \tag{7.6}$$

which simplifies into the required result.

Corollary 7.1.

$$\mathrm{Var}f(\Phi) = \lambda\,\mathbb{E}f^2\big(T_1^{(q)}\big). \tag{7.7}$$

Proof. Similarly as above it is easy to show that $\mathbb{E}f(\Phi) = \lambda\,\mathbb{E}f\big(T_1^{(q)}\big)$, and the result follows.

As a cursory check let $f(\Phi) = N$, the number of $q-$objects hitting the window W, see Eq. (7.3). Then $f\big(T_1^{(q)}\big) = f^2\big(T_1^{(q)}\big) \equiv 1$ and Eq. (7.7) yields

$$\mathrm{Var}N = \lambda, \tag{7.8}$$

as expected.

Suppose that Φ is isotropic, and let $f(\Phi) = \nu_q(\Phi \cap W)$, with $\nu_0(\Phi \cap W) \equiv N$, see Eq. (7.3). If Φ is a $q-$flat process, then applying Corollary 2.1 to Corollary 7.1 and recalling the first Eq. (7.4) we obtain,

$$\mathrm{Var}\{\nu_q(\Phi \cap W)\} = \begin{cases} \lambda_\Phi \displaystyle\int_0^\infty q b_q r^{q-1} k_W(r)\,\mathrm{d}r, & q = 1, 2, ..., n-1, \\ \lambda_\Phi\,\nu_n(W), & q = 0. \end{cases} \tag{7.9}$$

On the other hand, if Φ is an isotropic $q-$plate process, then applying Corollary 3.2 to Corollary 7.1 and recalling the second Eq. (7.4) we obtain,

$$\mathrm{Var}\{\nu_q(\Phi\cap W)\} = \lambda_\Phi\,\nu_q^{-1}\big(T_1^{(q)}\big)\int_0^\infty q b_q r^{q-1} k_W(r)\,k_{T_1^{(q)}}(r)\,\mathrm{d}r. \tag{7.10}$$

7.3 Special cases: isotropic Poisson line and line segment processes in $\mathbb{R}^2$

Isotropic Poisson line process in $\mathbb{R}^2$. On line with the two alternative interpretations of the intensity λ_Φ given in Subsection 7.1, we can consider two natural estimators of λ_Φ based on the intersection of Φ with a convex window W namely the counting estimator

$$\widehat{\lambda}_\Phi = \frac{\pi N}{\nu_1(\partial W)}, \qquad \mathrm{Var}\widehat{\lambda}_\Phi = \lambda_\Phi\frac{\pi}{\nu_1(\partial W)}, \tag{7.11}$$

and the direct estimator

$$\widetilde{\lambda}_\Phi = \frac{\nu_1(\Phi\cap W)}{\nu_2(W)}, \qquad \mathrm{Var}\widetilde{\lambda}_\Phi = \frac{\lambda_\Phi}{\nu_2^2(W)}\int_0^\infty 2k_W(r)\,\mathrm{d}r, \tag{7.12}$$

respectively. The expression for $\mathrm{Var}\widehat{\lambda}_\Phi$ follows on using Eq. (7.8), the first Eq. (7.4), and Cauchy's formula $\mathbb{E}_t\nu_1(W_t') = \nu_1(\partial W)/\pi$. On the other hand, $\mathrm{Var}\widetilde{\lambda}_\Phi$ follows from the first Eq. (7.9).

In particular, if W is a disk of diameter d we get,

$$\mathrm{Var}\widehat{\lambda}_\Phi = d^{-1}\lambda_\Phi \text{ and } \mathrm{Var}\widetilde{\lambda}_\Phi = \frac{32}{3\pi^2}d^{-1}\lambda_\Phi > \mathrm{Var}\widehat{\lambda}_\Phi, \tag{7.13}$$

respectively (for the second result we have used Eq. (2.9)). The preceding inequality is a particular case of Ohser's paradox, which is discussed in the next section.

Isotropic Poisson segment process in $\mathbb{R}^2$. Here the grains are isotropically oriented segments of length $l := \nu_1\big(T_1^{(1)}\big)$, and the germs are the midpoints of the segments which constitute a stationary and isotropic Poisson point process of intensity $\lambda_\Phi^{(0)}$, see Eq. (7.2). We consider two alternative unbiased estimators of λ_Φ based on the intersection of Φ with a convex window W. The first one is the counting estimator $\widehat{\lambda}_\Phi$, which is based on the number N of segments hitting W, and it uses the second Eq. (7.4). Thus,

$$\widehat{\lambda}_\Phi = \frac{Nl}{\mathbb{E}_t\nu_2\big(W_t\oplus\breve{T}_1^{(q)}\big)}, \qquad \mathrm{Var}\widehat{\lambda}_\Phi = \frac{l\lambda_\Phi}{\mathbb{E}_t\nu_2\big(W_t\oplus\breve{T}_1^{(q)}\big)}, \tag{7.14}$$

because $\mathbb{E}N = \mathrm{Var}N = \lambda = \lambda_\Phi l^{-1}\mathbb{E}_t\nu_2\big(W_t\oplus\breve{T}_1^{(0)}\big)$. The second estimator, $\widetilde{\lambda}_\Phi$, is the direct estimator, namely the ratio of the total segment length in the interior of W to the area of W. Thus,

$$\widetilde{\lambda}_\Phi = \frac{\nu_1(\Phi\cap W)}{\nu_2(W)}, \qquad \mathrm{Var}\widetilde{\lambda}_\Phi = \frac{\lambda_\Phi}{l\cdot\nu_2^2(W)}\int_0^\infty 2k_W(r)\,k_{T_1^{(1)}}(r)\,\mathrm{d}r, \tag{7.15}$$

the latter result stemming from Eq. (7.10).

To get explicit results suppose again that W is a disk of diameter d. Then,

$$\mathrm{Var}\widehat{\lambda}_\Phi = \frac{l\lambda_\Phi}{\pi d^2/4 + ld} \text{ and } \mathrm{Var}\widetilde{\lambda}_\Phi = \frac{\left(\frac{8}{3\pi}ld - \frac{1}{4}d^2\right)\lambda_\Phi}{\pi d^2 l/4} > \mathrm{Var}\widehat{\lambda}_\Phi, \tag{7.16}$$

respectively. For the second result we have applied Eq. (3.11) to the second Eq. (7.15) for the case $l > d$. As expected the preceding results converge to the corresponding ones in Eq. (7.13) as $l \to \infty$.

8. VARIANCE COMPARISONS FOR TWO DIFFERENT DESIGNS TO ESTIMATE THE INTENSITY OF A STATIONARY $q-$FLAT PROCESS

8.1 Paradoxes of Ohser type

Consider first a stationary and isotropic Poisson line process Φ with realizations in $\mathbb{R}^2$ sampled by a fixed convex window W, see Fig. 14. The inequality (7.13) shows that

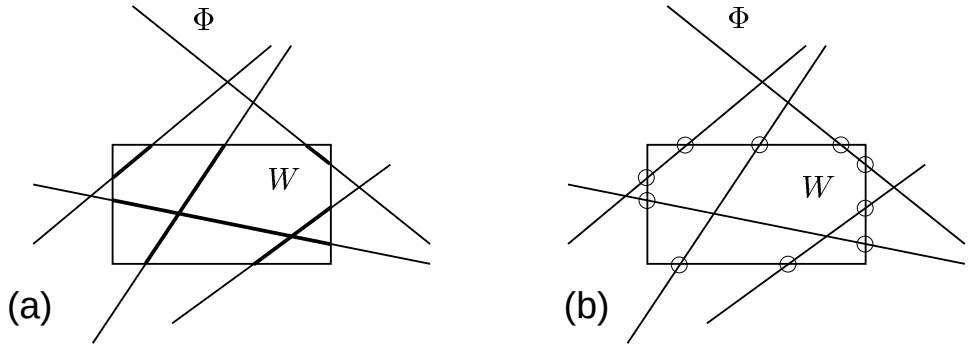

Figure 14 The Ohser type variance 'paradox' for Poisson lines on the plane. In order to estimate the intensity of the line process (namely the mean line length per unit area) with a convex window W, it is more efficient to count the number of test lines hitting the window (a) than the actual line length within the window (b). See Section 8.

$\mathrm{Var}\widetilde{\lambda}_\Phi > \mathrm{Var}\widehat{\lambda}_\Phi$ when W is a disk. More generally, for any convex window W we have

$$\mathbb{E}\{\nu_1(\Phi \cap W)|N\} = N \cdot \pi\nu_2(W)/\nu_1(\partial W), \tag{8.1}$$

so that, recalling the definitions given in Eq. (7.11) and Eq. (7.12),

$$\mathbb{E}\big(\widetilde{\lambda}_\Phi|N\big) = \pi N/\nu_1(\partial W) = \widehat{\lambda}_\Phi, \tag{8.2}$$

and by the Rao-Blackwell theorem,

$$\mathrm{Var}\widetilde{\lambda}_\Phi \geq \mathrm{Var}\mathbb{E}\big(\widetilde{\lambda}_\Phi|N\big) = \mathrm{Var}\widehat{\lambda}_\Phi. \tag{8.3}$$

Thus, for the stationary and isotropic Poisson line process the counting estimator (7.11) of the intensity λ_Φ is always at least as precise as the direct estimator (7.12), (Ohser, 1990). This is an apparent paradox because $\nu_1(\Phi \cap W)$ seems at the first sight to carry more information than N. On a second look, however, one realizes that the direct estimator has two sources of variation, the first one due the varying number of lines hitting W and the second due to the varying chord lengths within W, whereas the counting estimator has only the first source of variation.

Baddeley & Cruz-Orive (1995) revisited Ohser's paradox. Further, Schladitz (1999, 2000) proved the superior efficiency of the counting estimator $\widehat{\lambda}_\Phi$ of λ_Φ over the direct estimator $\widetilde{\lambda}_\Phi$ for a stationary Poisson $q-$flat process Φ with an arbitrary directional distribution, that is,

$$\widehat{\lambda}_\Phi = \frac{N}{\mathbb{E}_t \nu_{n-q}\big(W_t'\big)}, \;\; \widetilde{\lambda}_\Phi = \frac{\nu_q(\Phi \cap W)}{\nu_n(W)}, \;\; \operatorname{Var} \widehat{\lambda}_\Phi \leq \operatorname{Var} \widetilde{\lambda}_\Phi. \tag{8.4}$$

Below we show the same result using a simpler approach.

Lemma 8.1. Let $\widetilde{\lambda}_\Phi$ represent any unbiased estimator of λ_Φ. Then,

$$\mathbb{E}\big(\widetilde{\lambda}_\Phi | N\big) = \widehat{\lambda}_\Phi, \tag{8.5}$$

the counting estimator.

Proof. We use a similar argument and the same notation as in the proof of Proposition 7.1. Recall also that λ is given by the first Eq. (7.4). Thus,

$$\lambda_\Phi = \mathbb{E}\widetilde{\lambda}_\Phi = \sum_{k=0}^{\infty} p(k;\lambda)\, \mathbb{E}\big(\widetilde{\lambda}_\Phi | N = k\big), \; \forall \lambda \geq 0. \tag{8.6}$$

On the other hand,

$$\lambda_\Phi = \mathbb{E}\widehat{\lambda}_\Phi = \sum_{k=0}^{\infty} p(k;\lambda)\, \frac{k}{\mathbb{E}_t \nu_{n-q}\big(W_t'\big)}, \; \forall \lambda \geq 0. \tag{8.7}$$

From the preceding two identities it follows that

$$\sum_{k=0}^{\infty} \frac{\lambda^k}{k!}\, \mathbb{E}\big(\widetilde{\lambda}_\Phi | N = k\big) = \sum_{k=0}^{\infty} \frac{\lambda^k}{k!}\, \frac{k}{\mathbb{E}_t \nu_{n-q}\big(W_t'\big)}, \; \forall \lambda \geq 0. \tag{8.8}$$

Thus we have two identical power series in λ, and therefore the corresponding coefficients must be identical, whereby,

$$\mathbb{E}\big(\widetilde{\lambda}_\Phi | N = k\big) = \frac{k}{\mathbb{E}_t \nu_{n-q}\big(W_t'\big)} = 1_{\{N=k\}} \widehat{\lambda}_\Phi, \; \forall k \in \mathbb{N}, \tag{8.9}$$

which implies the required result.

Theorem 8.1. The counting estimator $\widehat{\lambda}_{\Phi}$ is the best unbiased estimator of the intensity λ_{Φ} of a stationary Poisson $q-$flat process Φ with an arbitrary directional distribution.

Proof. Bearing Lemma 8.1 in mind, the result is a direct consequence of the Rao-Blackwell theorem.

8.2 **Central limit theorems**

Let Φ_q represent the Poisson $q-$flat process of intensity λ_{Φ_q} in $\mathbb{R}^n$, generated by the intersections of $(n-q)-$tuples of hyperplanes of a stationary Poisson hyperplane process Φ_{n-1}. Suppose that Φ_{n-1} is sampled by a window $B_n(r)$, namely the $n-$dimensional ball of radius r, and consider the counting and the direct unbiased estimators of λ_{Φ_q}, namely

$$\widehat{\lambda}_{\Phi_q}(r) = \frac{\#(\Phi_q \cap B_n(r))}{\nu_{n-q}(B_{n-q}(r))}, \;\; \widetilde{\lambda}_{\Phi_q}(r) = \frac{\nu_q(\Phi_q \cap B_n(r))}{\nu_n(B_n(r))}, \tag{8.10}$$

respectively. Heinrich *et al.* (2006) have shown that the preceding estimators are asymptotically normally distributed and, moreover,

$$\lim_{r\to\infty} r\mathrm{Var}\big(\widehat{\lambda}_{\Phi_q}(r)\big) \leq \lim_{r\to\infty} r\mathrm{Var}\big(\widetilde{\lambda}_{\Phi_q}(r)\big), \tag{8.11}$$

namely the counting estimator is asymptotically more efficient than the direct estimator. Asymptotic confidence intervals were thereby constructed to estimate λ_{Φ_q} with the counting estimator.

9. DISCUSSION

In the foregoing sections we have presented a coherent set of second moment formulae for the intersections between bounded sets and flats, or test systems in Euclidean spaces. Some of these formulae were so far scattered in the literature, and even in these cases proofs were generally unavailable. The collection is however not exhaustive because we have assumed that the target set (or the sampling window in the model based case) was of dimension n in $\mathbb{R}^n$. More research is therefore needed to endow the subject with a bit more generality. In fact hitting a target set of dimension k with a probe of dimension q in $\mathbb{R}^n$ with $k+q \geq n$ but $k < n$ and $q < n$ is important for some applications. In particular it would be useful to predict the variance of the number of intersections between a target set consisting of curves and a known test system of curves in the plane (see e.g. Cruz-Orive & Gual-Arnau, 2002, Fig. 6 and 7).

The formulae are useful to compute second moments of intersection measures specially when the intersecting geometric objects are known analytically. For instance, a classical problem, already considered by Carl F. Gauss, is to determine the variance of the number of lattice points inside an randomly moving oval. The result of Eq. (4.13)

for the disk (Kellerer, 1986) is amenable to computation (Eq. (4.14)), easily extensible to the sphere, and it looks simpler than previous solutions (Kendall, 1948, Kendall & Rankin, 1953). In practical stereology, however, the problem is different: there one has for instance a bounded planar set of arbitrary shape, and the problem is to predict the variance of the point counting estimator of its area obtained with a test grid — or, one has a three dimensional object, like a brain, and the problem is to predict the variance of the Cavalieri estimator of volume (Matérn, 1960, 1989; Gundersen & Jensen, 1987; Cruz-Orive, 1989; Kiêu & Mora, 2006). The most popular practical approach is based on G. Matheron's transitive theory (Matheron, 1971; Kiêu *et al*., 1999; García-Fiñana & Cruz-Orive, 2004). In practice, however, the transitive approach is extensively used only for the point count estimator of area, and for the Cavalieri design. Technical difficulties arise when one tries to obtain variance predictors for other sampling schemes. In this sense, we feel that the formulae given here constitute prerequisites to progress in the mentioned direction. One has to rewrite them in a suitable way, eventually incorporating harmonic analysis, and seeking suitable models for the relevant geometric covariograms.

The formulae given here have also proved useful to better understand the so called 'paradoxes' arising when lower dimensional probes perform better that higher dimensional ones, both in the design case (Sections 5, 6) and in the model based case (Section 8). More work is needed, however, to establish new theorems — or at least new 'rules of thumb' — which better characterize such paradoxes, if at all possible, in a general setting.

ACKNOWLEDGMENTS

FV received an Erasmus grant to visit the University of Cantabria. LMCO acknowledges support from the Spanish Ministry of Education and Science I+D Project no. MTM2005–08689–C02–01.

REFERENCES

[1]. Baddeley, A. & Jensen, E.B.V. (2004) *Stereology for Statisticians*. Chapman & Hall/ CRC.

[2]. Baddeley, A.J. & Cruz-Orive, L.M. (1995) The Rao-Blackwell theorem in stereology and some counterexamples. *Adv. Appl. Probab.* **27**, 2–19.

[3]. Borel, E. & Lagrange, R. (1925) *Traité du Calcul des Probabilités et de ses Applications*. Gauthier-Villars, Paris.

[4]. Cochran, W.G. (1977) *Sampling Techniques*, 3rd edn. J. Wiley & Sons, New York.

[5]. Cruz-Orive, L.M. (1980) Best linear unbiased estimators for stereology. *Biometrics* **36**, 595–605.

[6]. Cruz-Orive, L.M. (1989). On the precision of systematic sampling: a review of Matheron's transitive methods. *J. Microsc.* **153**, 315–333.

[7]. Cruz-Orive, L.M. (2002) Stereology: meeting point of integral geometry, probability, and statistics. In memory of Profesor Luis A. Santaló (1911–2001). *Math. Notae* **41**, 49–98. Special issue, Homenaje a L.A. Santaló.

[8]. Cruz-Orive, L.M. (2003) Estereología: Punto de encuentro de la Geometría Integral, la Probabilidad y la Estadística. En memoria del Profesor Luis A. Santaló (1911–2001). *La Gaceta de la RSME* **6**, 469–513.

[9]. Cruz-Orive, L.M. (2006) A general variance predictor for Cavalieri slices. *J. Microsc.* **222**, 158–165.

[10]. Cruz-Orive, L.M. & Gual-Arnau, X. (2002) Precision of circular systematic sampling. *J. Microsc.* **207**, 225–242.

[11]. Davy, P.J. & Miles. R.E. (1977) Sampling theory for opaque spatial specimens. *J. Roy. Statist. Soc. B*, **39**, 56–65.

[12]. De-lin, R. (1994) *Topics in Integral Geometry*. World Scientific, Singapore.

[13]. Diggle, P.J. (2003) *Statistical Analysis of Spatial Point Patterns.* 2nd edn. Arnold, London.

[14]. Enns, E.G. & Ehlers, P.F. Random paths through a convex region. *J. Appl. Probab.* **15**, 144–152.

[15]. García-Fiñana, M. & Cruz-Orive, L.M. (2004) Improved variance prediction for systematic sampling on $\mathbb{R}$. *Statistics* **38**, 243–272.

[16]. Ghosh, B. (1943) On the distribution of random distances in a rectangle. *Science and Culture* **8**, 388.

[17]. Gual Arnau, X. & Cruz-Orive, L.M. (1998) Variance prediction under systematic sampling with geometric probes. *Adv. Appl. Probab.* **30**, 889–903.

[18]. Gual-Arnau, X. & Cruz-Orive, L.M. (2006) New variance expressions for systematic sampling: the filtering approach. *J. Microsc.* **222**, 217–227.

[19]. Gundersen, H.J.G. & Jensen, E.B. (1987) The efficiency of systematic sampling in stereology and its prediction. *J. Microsc.* **147**, 229–263.

[20]. Heinrich L., Schmidt H. & Schmidt V. (2006) Central limit theorems for Poisson hyperplane tessellations. *Ann. Appl. Prob.* **16**, 919-950.

[21]. Howard, C.V. & Reed, M.G. (1998) *Unbiased Stereology. Three-dimensional Measurement in Microscopy.* Bios, Oxford.

[22]. Jensen, E.B. & Gundersen, H.J.G. (1982) Stereological ratio estimation based on counts from integral test systems. *J. Microsc.* **125**, 51–66.

[23]. Kellerer, A.M. (1986) The variance of a Poisson process of domains. *J. Appl. Probab.* **23**, 307–321.

[24]. Kendall, D.G. (1948) On the number of lattice points inside a random oval. *Quart. J. Math.* **4**, 178–189.

[25]. Kendall, D.G. & Rankin, R.A. (1953) On the number of points of a given lattice in a random hypersphere. *Quart. J. Math. Oxford* **4**, 178–189.

[26]. Kiêu, K. & Mora, M. (2006) Precision of stereological planar area predictors. *J. Microsc.* **222**, 201–211.

[27]. Kiêu, K., Souchet, S. & Istas, J. (1999) Precision of systematic sampling and transitive methods. *J. Statist. Plan. Inf.* **77**, 263–279.

[28]. Matérn, B. (1960) *Spatial Variation*, Reprinted in 1986 as 2nd edn. Lecture Notes in Statistics, 36. Springer-Verlag, Berlin.

[29]. Matérn, B. (1989) Precision of area estimation: a numerical study. *J. Microsc.* **153**, 269–284.

[30]. Matheron, G. (1971) *The Theory of Regionalized Variables and Its Applications.* Les Cahiers du Centre de Morphologie Mathématique de Fontainebleau, No. 5. École Nationale Supérieure des Mines de Paris, Fontainebleau.

[31]. Matheron, G. (1975) *Random Sets and Integral Geometry*. J. Wiley & Sons, New York.

[32]. Mecke, J. (1981) Stereological formulas for manifold processes. *Probab. Math. Statist.* **2**, 31–35.

[33]. Mecke, J., Schneider, R., Stoyan, D. & Weil, W. (1990) *Stochastische Geometrie*. Birkhäuser, Basel.

[34]. Miles, R.E. (1964) Random polygons determined by random lines in a plane. *Proc. Nat. Acad. Sci.* **52**, 901–907. II, 1157–1160.

[35]. Miles, R.E. (1972) Multidimensional perspectives in stereology. *J. Microsc.* **95**, 181–195.

[36]. Miles, R.E. (1974) A synopsis of 'Poisson flats in Euclidean spaces'. In: *Stochastic Geometry*, ed. by E.F. Harding and D. G. Kendall. Wiley, New York.

[37]. Miles, R.E. & Davy, P.J. (1976) Precise and general conditions for the validity of a comprehensive set of stereological fundamental formulae. *J. Microsc.* **107**, 211–226.

[38]. Ohser, J. (1990) *Grundlagen und praktische Möglichkeiten der Charakterisierung struktureller Inhomogeneitäten von Werkstoffen.* Dr. sci. tech. thesis, Bergakademie Freiberg.

[39]. Ripley, B.D. (1981) *Spatial Statistics.* J. Wiley & Sons, New York.

[40]. Santaló, L.A. (1976) *Integral Geometry and Geometric Probability*. Addison-Wesley, Reading, Massachusetts.

[41]. Schladitz, K. (1996) *Estimation of the Intensity of Stationary Flat Processes*. PhD thesis, Friedrich-Schiller Universität Jena.

[42]. Schladitz, K. (1999) Surprising optimal estimators for the area fraction. *Adv. Appl. Probab.* **31**, 995–1001.

[43]. Schladitz, K. (2000) Estimation of the intensity of stationary flat processes. *Adv. Appl. Probab.* **32**, 114–139.

[44]. Stoyan, D., Kendall, W.S. & Mecke, J. (1995) *Stochastic Geometry and its Applications.* 2nd. ed. J. Wiley & Sons, Chichester.

[45]. Voss, F. (2005) *First and Second Moment Measures in Geometric Sampling for Stereology.* Diploma thesis, Abteilung Stochastik, Universität Ulm.

[46]. Weibel, E.R. (1979) *Stereological Methods. Vol. 1: Practical Methods for Biological Morphometry.* Academic Press, London.

Appendix A. BASIC TOOLS FOR GEOMETRIC SAMPLING

A.1 Unbounded flat probes

Let $G_{q,n-q}$ denote the Grassmann manifold, namely the space of non-oriented linear $q-$subspaces $L_{q[0]}$ in $\mathbb{R}^n$, and let $F_{n,q}$ denote the space of $q-$flats L_q. For a vector $z \in \mathbb{R}^n$ we have,

$$L_q = L_{q[0]} + z, \;\; z \in L_{q[0]}^{\perp} = L_{n-q[0]}, \;\; q = 0, 1, ..., n, \tag{A.1}$$

(a 0–flat is just a point). Thus, a $q-$flat is a linear $q-$subspace translated by a vector z from its unique orthogonal complement $L_{q[0]}^{\perp}$, which is in fact a linear $(n-q)-$subspace. The density $\mathrm{d}L_{q[0]}$ of the rotation-invariant measure on $G_{q,n-q}$ is unique up to a constant factor (Santaló, 1976). Moreover, $\mathrm{d}L_{q[0]} = \mathrm{d}L_{n-q[0]}$. On the other hand, the density $\mathrm{d}L_q$ of the motion-invariant measure on $F_{n,q}$ may be expressed as follows,

$$\mathrm{d}L_q = \nu_{n-q}(\mathrm{d}z) \wedge \mathrm{d}L_{n-q[0]}, \tag{A.2}$$

namely the exterior product of the density of the Lebesgue measure in the orthogonal complement of L_q (which is responsible for the location of L_q), times the invariant density for the orthogonal complement, (which is responsible for the orientation of L_q).

Stereology and stochastic geometry incorporate probability theory and statistics to the foregoing concepts of integral geometry (Miles & Davy, 1976, see Cruz-Orive, 2002, 2003 for a survey). The first step is to construct probability elements induced by the relevant invariant densities. For instance the rotation-invariant or isotropic probability element on $G_{q,n-q}$ reads,

$$\mathbb{P}(\mathrm{d}t) = \frac{\mathrm{d}t}{\displaystyle\int_{G_{q,n-q}} \mathrm{d}t}, \;\; t \in G_{q,n-q}. \tag{A.3}$$

where we write $\mathrm{d}t$ for $\mathrm{d}L_{q[0]}$, for short. When convenient, we also write $L_q(z,t)$ for the $r-$flat which is a translation of $L_{q[0]} \equiv L_q(0,0)$ by z. The denominator of the normalizing constant in the right hand side of Eq. (A.3) is the total measure of $G_{q,n-q}$, namely,

$$\int_{G_{q,n-q}} \mathrm{d}t \equiv \int_{G_{q,n-q}} \mathrm{d}L_{q[0]} = \frac{O_{n-1}O_{n-2}\cdots O_{n-q}}{O_{q-1}O_{q-2}\cdots O_0}, \tag{A.4}$$

where O_k is the surface area of the $k-$dimensional unit sphere $\mathbb{S}^k$, see Appendix D. Thus $\mathbb{P}(\mathrm{d}t)$ may be regarded as a uniform probability element on $G_{q,n-q}$. On the other hand the measure on $F_{n,q}$ is not finite, and consequently we may resort to defining a probability element for $q-$flats hitting a compact $n-$dimensional subset $Y \subset \mathbb{R}^n$, whereby the denominator of the normalizing constant is,

$$\begin{aligned}\int_{\{L_q : Y \cap L_q \neq \emptyset\}} \mathrm{d}L_q &= \left(\int_{G_{q,n-q}} \mathrm{d}t\right) \int_{G_{q,n-q}} \mathbb{P}(\mathrm{d}t) \int_{Y_t'} \nu_{n-q}(\mathrm{d}z) \\ &= \left(\int_{G_{q,n-q}} \mathrm{d}t\right) \mathbb{E}_t \nu_{n-q}(Y_t'),\end{aligned} \tag{A.5}$$

where Y_t' represents the orthogonal projection of Y onto the orthogonal complement of $t \in G_{q,n-q}$. Thus the probability element for a isotropic and uniform random $q-$flat ('IUR $q-$flat', an abbreviation introduced by R.E. Miles) hitting Y reads,

$$\mathbb{P}(\mathrm{d}z, \mathrm{d}t|\uparrow) := \mathbb{P}(\mathrm{d}z, \mathrm{d}t | Y \cap L_q(z,t) \neq \emptyset) = \frac{\nu_{n-q}(\mathrm{d}z)\,\mathbb{P}(\mathrm{d}t)}{\mathbb{E}_t \nu_{n-q}(Y_t')}. \tag{A.6}$$

The preceding expression is valid for a directional distribution $\mathbb{P}(\cdot)$ which is not necessarily isotropic. In particular, if the direction t is constant the $q-$flat is said to be FUR (fixed uniform random) hitting Y. The corresponding probability element is that of the uniform distribution on Y_t' namely,

$$\mathbb{P}(\mathrm{d}z|t,\uparrow) = \frac{\nu_{n-q}(\mathrm{d}z)}{\nu_{n-q}(Y_t')}, \quad z \in Y_t'. \tag{A.7}$$

Moreover, dividing the right hand side of Eq. (A.6) by that of (A.7) we obtain,

$$\mathbb{P}(\mathrm{d}t|\uparrow) = \frac{\nu_{n-q}(Y_t')\,\mathbb{P}(\mathrm{d}t)}{\mathbb{E}_t \nu_{n-q}(Y_t')}, \quad t \in G_{q,n-q}. \tag{A.8}$$

The mean contents of the intersection between a $k-$dimensional subset $Y_k \subset \mathbb{R}^n$ and a IUR $q-$flat $L_q(z,t)$ hitting Y_k is easy to determine using the Crofton-Santaló formula (Santaló, 1976, p. 245; De-lin, 1994, p. 157) and Eq. (A.6) with Eq. (A.3). Here and in the sequel we assume that $k+q \geq n$. The result is,

$$\mathbb{E}\nu_{k+q-n}\big(Y_k \cap L_q(z,t)|\uparrow\big) = \frac{1}{\mathbb{E}_t \nu_{n-q}\big((Y_k)_t'\big)} \cdot \frac{O_n O_{k+q-n}}{O_k O_q} \cdot \nu_k(Y_k). \tag{A.9}$$

For $k = n$ we have the following formula for a FUR $q-$flat hitting Y_n,

$$\mathbb{E}\nu_q\big(Y_n \cap L_q(z,t)|t,\uparrow\big) = \frac{\nu_n(Y_n)}{\nu_{n-q}\big((Y_n)'_t\big)}. \tag{A.10}$$

Suppose that Y_n is a convex body and set $k = n-1$, $q = 1$. Then the left hand side of Eq. (A.9) is almost surely equal to 2 and we get Cauchy's projection formula,

$$\mathbb{E}_t\nu_{n-1}\big((Y_{n-1})'_t\big) = \frac{O_nO_0}{2\,O_{n-1}O_1}\cdot\nu_{n-1}(Y_{n-1}). \tag{A.11}$$

For instance the mean orthogonal projected length of a convex set $Y_2 \subset \mathbb{R}^2$ onto an isotropic axis is $\nu_1(\partial Y)/\pi$; the mean orthogonal projected area of a convex set $Y_3 \subset \mathbb{R}^3$ onto an isotropic plane is $\nu_2(\partial Y)/4$; etc.

Many first order formulae emerge by combining the foregoing results. In fact, Eq. (A.9), together with Eq. (A.21) below, constitute the building bricks of the 'fundamental equations of stereology'.

A.2 **Bounded probes: the kinematic measure**

In the preceding section we have described IUR $q-$flats as probes hitting a given compact set $Y \subset \mathbb{R}^n$. Here we consider instead a bounded $q-$probe, namely a bounded manifold $T \subset \mathbb{R}^n$ of dimension $q = 0, 1, ..., n$. With T we associate a point $x \in T$ and an orthogonal $n-$frame with the origin at x and rigidly attached to T. When the $n-$frame is the reference frame centred at the origin the $q-$probe will be denoted by $T^{(q)}_{0,0}$, or $T_{0,0}$ simply if the dimension is understood. Let G_n denote the special group of motions in $\mathbb{R}^n$. A motion $g \in G_n$ of $T_{0,0}$ is a composition of a translation of $T_{0,0}$ by a vector $x \in \mathbb{R}^n$, (whereby we can write $T_{x,0} = T_{0,0} + x$), with an independent rotation $t \in G_{n[x]}$ about x. Here $G_{n[x]}$ denotes the special group of rotations acting upon the $n-$frame associated with $T_{x,0}$. The special group $G_{n[x]}$ is isomorphic with $SO(n)$, and its invariant density is

$$\mu_{[x]}(\mathrm{d}t) = \mathrm{d}u_{n-1} \wedge \mathrm{d}u_{n-2} \wedge \cdots \wedge \mathrm{d}u_1, \;\; t \in G_{n[x]}, \;\; u_k \in \mathbb{S}^k, \tag{A.12}$$

where $\mathrm{d}u_k$ is the area element on $\mathbb{S}^k$. Therefore,

$$\int_{G_{n[0]}} \mu_{[0]}(\mathrm{d}t) = O_{n-1}O_{n-2}\cdots O_1. \tag{A.13}$$

Summarizing, for the transform of $T_{0,0}$ by g we use the following notation,

$$g\,T_{0,0} = T_{x,t}, \;\; g = (x,t) \in G_n, \;\; x \in \mathbb{R}^n, \;\; t \in G_{n[x]}. \tag{A.14}$$

The required invariant density is the volume element of G_n, and it called the *kinematic density* of Blaschke-Santaló. Its expression reads

$$\mu(\mathrm{d}g) = \nu_n(\mathrm{d}x) \wedge \mu_{[x]}(\mathrm{d}t), \;\; g \in G_n. \tag{A.15}$$

By virtue of Eq. (A.13) the invariant probability element for a rotation about the origin can be written

$$\mathbb{P}(\mathrm{d}t) = \frac{\mu_{[0]}(\mathrm{d}t)}{O_{n-1}O_{n-2}\cdots O_1}, \;\; t \in G_{n[0]}. \tag{A.16}$$

Since the measure $\mu(G_n)$ is not finite we may restrict ourselves to bounded sets of G_n. For instance, for a $n-$dimensional compact set $Y \subset \mathbb{R}^n$ we have,

$$\mu\big(\{g \in G_n : Y \cap gT_{0,0} \neq \emptyset\}\big) = O_{n-1}O_{n-2}\cdots O_1\, \mathbb{E}_t\nu_n\big(Y \oplus \breve{T}_{0,t}\big). \tag{A.17}$$

Now the invariant probability element for all motions $g = (x,t)$ which bring $T_{0,0}$ into $T_{x,t}$ such that the event $\uparrow := Y \cap T_{x,t} \neq \emptyset$ holds, becomes

$$\mathbb{P}(\mathrm{d}x, \mathrm{d}t|\uparrow) = \frac{\nu_n(\mathrm{d}x)\,\mathbb{P}(\mathrm{d}t)}{\mathbb{E}_t\nu_n\big(Y \oplus \breve{T}_{0,t}\big)}. \tag{A.18}$$

and we say that $T_{x,t}$ is a IUR $q-$probe hitting Y. For a FUR $q-$probe hitting Y,

$$\mathbb{P}(\mathrm{d}x|t,\uparrow) = \frac{\nu_n(\mathrm{d}x)}{\nu_n\big(Y \oplus \breve{T}_{0,t}\big)}, \;\; x \in Y \oplus \breve{T}_{0,t}, \tag{A.19}$$

the uniform distribution. Furthermore,

$$\mathbb{P}(\mathrm{d}t|\uparrow) = \frac{\nu_n\big(Y \oplus \breve{T}_{0,t}\big)\,\mathbb{P}(\mathrm{d}t)}{\mathbb{E}_t\nu_n\big(Y \oplus \breve{T}_{0,t}\big)}, \;\; t \in G_{n[0]}. \tag{A.20}$$

To calculate the mean contents of the intersection between a $k-$dimensional subset $Y_k \subset \mathbb{R}^n$ and a bounded IUR $q-$probe $T_{x,t}$ hitting it we may use the Santaló formula for bounded sets (Santaló, 1976, p. 259; De-lin, 1994, p. 161) and Eq. (A.18) with Eq. (A.16). Thus,

$$\mathbb{E}\nu_{k+q-n}\big(Y_k \cap T_{x,t}|\uparrow\big) = \frac{1}{\mathbb{E}_t\nu_n\big(Y_k \oplus \breve{T}_{0,t}\big)} \cdot \frac{O_nO_{k+q-n}}{O_kO_q} \cdot \nu_k(Y_k)\,\nu_q(T_{0,0}). \tag{A.21}$$

For $k = n$ we obtain the following formula for a bounded FUR $q-$probe hitting Y_n,

$$\mathbb{E}\nu_q\big(Y_n \cap T_{x,t}|t,\uparrow\big) = \frac{\nu_n(Y_n)\,\nu_q(T_{0,0})}{\nu_n\big(Y_n \oplus \breve{T}_{0,t}\big)}. \tag{A.22}$$

Neither Eq. (A.21) nor Eq. (A.9) are used directly in stereology for estimation purposes because the respective right hand sides depend on the unknown set Y_k. Nonetheless it is opportune to mention that $\mathbb{E}_t\nu_n\big(Y_n \oplus \breve{T}_{0,t}\big)$ can be computed in some cases (notably if $Y_n \cap T_{x,t}$ is simply connected for all $(x,t) \in G_n$) by means of the kinematic formula of Blaschke-Santaló (Santaló, 1976, p. 262). For instance if $Y,\, T \subset \mathbb{R}^2$ are planar convex sets, then,

$$\mathbb{E}_t\nu_2\big(Y \oplus \breve{T}\big) = \nu_2(Y) + \nu_2(T) + (2\pi)^{-1}\nu_1(\partial Y)\,\nu_1(\partial T). \tag{A.23}$$

A.3 **Test systems**

A probe which opens the way to applications in stereology is the test system (of bounded $q-$probes, or of $q-$flats). Details can be found in Santaló (1976, Ch. 8).

A test system of bounded $q-$probes may be constructed as follows.

(1). Choose a *fundamental tile* for a partition of $\mathbb{R}^n$, namely a bounded subset $J_{0,0} \subset \mathbb{R}^n$ satisfying the following properties,

$$\exists \tau_{k,0} \in \mathbb{R}^n : \quad \mathbb{R}^n = \bigcup_{k\in\mathbb{Z}} J_{\tau_{k,0},0}, \;\; J_{\tau_{k,0},0} \cap J_{\tau_{l,0},0} = \emptyset \text{ if } \; k \neq l, \tag{A.24}$$

where $J_{z,0}$ is the translate of $J_{0,0}$ by $z \in \mathbb{R}^n$.

(2). Choose a basic probe $T_{0,0}$ of dimension q which is contained in $J_{0,0}$, whereby we obtain the following periodic set

$$\Lambda_{0,0} = \bigcup_{k\in\mathbb{Z}} T_{\tau_{k,0},0}. \tag{A.25}$$

(3). Apply an isotropic and uniform random motion $g \equiv (x,t) \in G_n$ to $\Lambda_{0,0}$ to obtain the required construction $g\Lambda_{0,0} = \Lambda_{x,t}$ as follows. First rotate the fundamental tile $J_{0,0}$ by $t \in G_{n[0]}$ with the isotropic probability element (A.16), to obtain $J_{0,t}$; with this fundamental tile obtain an isotropically rotated partition with tiles $J_{\tau_{k,t},t} = J_{0,t} + \tau_{k,t}$, where $\tau_{k,t}$ is the translation vector $\tau_{k,0}$ rotated about the origin. The probes $T_{\tau_{k,0},0}$ are rotated with the tiles containing them to get $T_{\tau_{k,t},t}$. Finally choose a uniform random point $x \in J_{0,t}$, so that the joint probability element of the pair (x,t) is

$$\mathbb{P}(\mathrm{d}x, \mathrm{d}t) = \frac{\mu_{[0]}(\mathrm{d}t)}{O_{n-1}O_{n-2}\cdots O_1} \cdot \frac{\nu_n(\mathrm{d}x)}{\nu_n(J_{0,0})}, \;\; t \in G_{n[0]}, \; x \in J_{0,t}. \tag{A.26}$$

Then

$$\Lambda_{x,t} = \bigcup_{k\in\mathbb{Z}} T_{x+\tau_{k,t},t}, \tag{A.27}$$

is a IUR test system.

Consider an unknown $k-$dimensional compact set $Y_k \subset \mathbb{R}^n$. The fundamental advantage of test systems is that, unlike Eq. (A.6) and (A.18), the probability element (A.26) does not depend on Y_k. Using Santaló's identity (Santaló, 1976, p. 131; see also Cruz-Orive, 2002, 2003) we obtain,

$$\mathbb{E}\nu_{k+q-n}(Y_k \cap \Lambda_{x,t}) = \frac{O_n O_{k+q-n}}{O_k O_q} \cdot \frac{\nu_q(T_{0,0})}{\nu_n(J_{0,0})} \cdot \nu_k(Y_k). \tag{A.28}$$

The generation of a test system of $q-$flats follows similar steps as above.

(1). Choose an isotropic $(n-q)-$subspace $L_{n-q}(0,t)$ with $t \in G_{q,n-q}$ according to the probability element (A.3).

(2). Choose a fundamental tile $J_{0,t}$ of $L_{n-q}(0,t)$ and construct the corresponding periodic set

$$\Lambda_{0,t} = \bigcup_{k\in\mathbb{Z}} L_q(\tau_{k,t}, t), \tag{A.29}$$

where $-\tau_{k,t}$ is a translation vector which brings $J_{\tau_{k,t},t}$ to coincide with $J_{0,t}$ leaving $\Lambda_{0,t}$ unchanged for all $k \in \mathbb{Z}$.

(3). Finally choose a uniform random point $z \in J_{0,t}$ so that the joint probability element of the pair (z,t) is,

$$\mathbb{P}(\mathrm{d}z, \mathrm{d}t) = \frac{\nu_{n-q}(\mathrm{d}z)\,\mathbb{P}(\mathrm{d}t)}{\nu_{n-q}(J_{0,0})}, \;\; z \in J_{0,t},\; t \in G_{q,n-q}, \tag{A.30}$$

where $\mathbb{P}(\mathrm{d}t)$ is the isotropic density (A.3). We thereby obtain the required IUR test system of $q-$flats

$$\Lambda_{z,t} = \bigcup_{k\in\mathbb{Z}} L_q(z+\tau_{k,t}, t). \tag{A.31}$$

For a IUR test system of $q-$flats we have the corresponding identity,

$$\mathbb{E}\nu_{k+q-n}(Y_k \cap \Lambda_{z,t}) = \frac{O_n O_{k+q-n}}{O_k O_q} \cdot \frac{1}{\nu_{n-q}(J_{0,0})} \cdot \nu_k(Y_k). \tag{A.32}$$

A.4 **The geometric covariogram**

Let Y denote a compact $n-$dimensional set of $\mathbb{R}^n$ and $x = (r,u) \in \mathbb{R}^n$ a point or vector of modulus $r = ||x||$ and orientation $u \in \mathbb{S}^{n-1}$. The geometric covariogram of the set Y is defined as

$$k_Y(x) = \int_{\mathbb{R}^n} 1_Y(y)\, 1_Y(y+x)\, \nu_n(\mathrm{d}y), \;\; x \in \mathbb{R}^n, \tag{A.33}$$

(Matheron, 1971), and it has the following properties,

$$\begin{aligned}
&k_Y(x) = \nu_n(Y \cap Y_{-x}), \text{ where } Y_{-x} := Y - x,\\
&k_Y(x) = k_Y(-x),\\
&k_Y(0) = \nu_n(Y) \geq k_Y(x) \geq k_Y(\infty) = 0, \; \forall x \in \mathbb{R}^n,\\
&\int_{\mathbb{R}^n} k_Y(x)\,\mathrm{d}x = \nu_n^2(Y).
\end{aligned} \tag{A.34}$$

If we average $k_Y(x)$ over isotropic rotations, namely with respect to the isotropic orientation density

$$\mathbb{P}(\mathrm{d}u) = \frac{\mathrm{d}u}{O_{n-1}}, \quad u \in \mathbb{S}^{n-1}, \tag{A.35}$$

then we obtain the isotropic geometric covariogram

$$k_Y(r) = \mathbb{E}_u k_Y(r,u) = \int_{\mathbb{S}^{n-1}} k_Y(r,u)\, \mathbb{P}(\mathrm{d}u), \quad r \geq 0. \tag{A.36}$$

Examples of isotropic geometric covariograms

For a disk $Y \subset \mathbb{R}^2$ of diameter d we have, (Borel & Lagrange, 1925),

$$\begin{aligned} &k_{disk}(r,d) = d^2\, g_{disk}(r/d), \\ &g_{disk}(x) = \begin{cases} \frac{1}{2}\big(\cos^{-1} x - x\sqrt{1-x^2}\big), & (0 \leq x \leq 1), \\ 0, & (1 < x < \infty). \end{cases} \end{aligned} \tag{A.37}$$

For a square $Y \subset \mathbb{R}^2$ of side length s we have, (Ghosh, 1943),

$$\begin{aligned} &k_{sq,k}(r,s) = s^2\, g_{sq,k}(r/s), \quad k = 1,2,3, \\ &\begin{cases} g_{sq,1}(x) = \big(\pi - 4x + x^2\big)/\pi, & (0 \leq x \leq 1), \\ g_{sq,2}(x) = \big(4\sin^{-1}(1/x) + 4\sqrt{x^2-1} - x^2 - 2 - \pi\big)/\pi, & \big(1 \leq x \leq \sqrt{2}\big), \\ g_{sq,3}(x) = 0, & \big(\sqrt{2} < x < \infty\big). \end{cases} \end{aligned} \tag{A.38}$$

Finally, for a straight line segment $Y \subset \mathbb{R}^2$ of length l,

$$k_{seg}(r,l) = \begin{cases} l - r, & (0 \leq r \leq l), \\ 0, & (l < r < \infty). \end{cases} \tag{A.39}$$

Appendix B. ELEMENTS OF STOCHASTIC GEOMETRY FOR MODEL BASED STEREOLOGY

B.1 Manifold processes

As described in Mecke (1981), a $q-$dimensional manifold process is a random variable Φ defined on a probability space $(\Omega, \mathcal{F}, \mathbb{P})$ with values in $(\mathbb{M}_q, \mathcal{M}_q)$, where:

- $\mathbb{M}_q$ is the family of closed sets $\varphi \subset \mathbb{R}^n$ with the property that the intersection with a ball $B_n(x,r)$ is a piecewise smooth $q-$dimensional manifold of class C^1 and

$$\nu_k(\varphi \cap B_n(x,r)) < \infty, \quad \forall r > 0,\ x \in \mathbb{R}^n. \tag{B.1}$$

- $\mathcal{M}_q$ is the smallest $\sigma-$algebra in $\mathbb{M}_q$ such that all functions f_B of the form

$$f_B : \mathbb{M}_q \to \mathbb{R} :\ f_B(\varphi) = \nu_q(\varphi \cap B) \tag{B.2}$$

are measurable $\forall B \in \mathcal{B}(\mathbb{R}^n)$, where $\mathcal{B}(\mathbb{R}^n)$ is the Borel $\sigma-$algebra in $\mathbb{R}^n$.

Thus the distribution $\mathbb{P}_\Phi$ of Φ is a probability measure on $(\mathbb{M}_q, \mathcal{M}_q)$, and the choice of $\mathcal{M}_q$ ensures that $\nu_q(\Phi \cap B)$ is a real random variable $\forall B \in \mathcal{B}(\mathbb{R}^n)$.

A manifold process Φ is called stationary if it has the same distribution as its translate Φ_z, $\forall z \in \mathbb{R}^n$, that is if $\mathbb{P}_\Phi$ is translation invariant. Further Φ is isotropic if it has the same distribution as its rotation $t\Phi$, $\forall t \in G_{n[0]}$, that is if $\mathbb{P}_\Phi$ is rotation invariant. If Φ is both stationary and isotropic, then $\mathbb{P}_\Phi$ is said to be motion invariant. An important characteristic of a manifold process Φ is its intensity λ_Φ, namely

$$\lambda_\Phi = \frac{\mathbb{E}\nu_q(\Phi \cap B)}{\nu_n(B)} \text{ for } B \in \mathbb{M}_q,\ \nu_n(B) < \infty. \tag{B.3}$$

Examples of manifold processes are point processes $(q = 0)$ and line or fibre processes $(q = 1)$. Manifold processes are special cases of random closed sets (Matheron, 1975; Mecke *et al.*, 1990; Stoyan *et al.*, 1995).

B.2 **Stationary Poisson processes of points, $q-$flats, and $q-$subsets**

A stationary Poisson point process Φ of intensity λ in $\mathbb{R}^n$ is characterized by the following two properties:

- the random variable $\nu_0\big(B \cap \Phi\big)$ has Poisson distribution with mean $\lambda\nu_n(B)$ $\forall B \in \mathcal{B}(\mathbb{R}^n)$,
- the random variables $\nu_0\big(B_1 \cap \Phi\big), ..., \nu_0\big(B_k \cap \Phi\big)$ are independent for all disjoint $B_1, ..., B_k \in \mathcal{B}(\mathbb{R}^n)$ and arbitrary $k \in \mathbb{N}$.

A relevant consequence is that, if $\nu_0(B \cap \Phi) = N$ for a compact set $B \subset \mathbb{R}^n$, then the N points are uniform and independent in B.

A stationary Poisson $q-$flat process (Miles, 1974) is a manifold process

$$\Phi = \bigcup_{k \in \mathbb{N}} L_q(z_k, t_k) \tag{B.4}$$

of intensity λ_Φ in $\mathbb{R}^n$ such that:

- the translations $\bigcup_{k\in\mathbb{N}} z_k$ form a stationary Poisson point process of intensity λ_Φ in $\mathbb{R}^{n-q}$,
- the orientations $(t_1, t_2, ...)$, $t_k \in G_{q,n-q}$ $\forall k \in \mathbb{N}$ are independent and identically distributed.

For a compact $k-$dimensional window $Y_k \subset \mathbb{R}^n$ with $k + q \geq n$ we have the following first order formula, (analogous to Eq. (A.32)),

$$\mathbb{E}\nu_{k+q-n}\big(\Phi \cap Y_k\big) = \lambda_\Phi \cdot \frac{O_n O_{k+q-n}}{O_k O_q} \cdot \nu_k(Y_k), \tag{B.5}$$

(Mecke, 1981).

Finally, a stationary Poisson process of congruent $q-$dimensional subsets (or $q-$subsets, for short) $T^{(q)}_{z_k,t_k}$ is a manifold process

$$\Phi = \bigcup_{k\in\mathbb{N}} T^{(q)}_{z_k,t_k} \tag{B.6}$$

of intensity λ_Φ in $\mathbb{R}^n$ such that:

• the translations $\bigcup_{k\in\mathbb{N}} z_k$ form a stationary Poisson point process in $\mathbb{R}^n$ of intensity

$$\lambda^{(0)}_\Phi = \lambda_\Phi / \nu_q\big(T^{(q)}_{z_1,k_1}\big), \;\; q < n, \tag{B.7}$$

• the rotations $(t_1, t_2, ...),\ t_k \in G_{n[0]}\ \ \forall k \in \mathbb{N}$ are independent and identically distributed.

Here Φ is also called a germ-grain process with Poisson germs, (Stoyan *et al.*, 1995). For a compact $k-$dimensional window $Y_k \subset \mathbb{R}^n$ the same identity (B.5) holds also in this case (by analogy with Eq. (A.28)).

Appendix C. DETAILS FOR THE COMPUTATION OF SECOND MOMENTS

C.1 Square hit by the boundary of another square.

We specify the limits of the double integrals in the right hand side of Eq. (3.18) to facilitate their numerical computation for the corresponding plot in Fig. 9. The different ranges of variation of the side lengths d, s of object and probe, respectively, and the actual domains of variation of $k_{sq,1}, k_{sq,2}$, (Eq. (A.38)), lead to the following expressions,

$$\begin{aligned}
&\frac{1}{8}\,\mathbb{E}_t\nu_2\big(Y \oplus \breve{T}_{0,t}\big)\cdot \mathbb{E}\nu_1^2\big(Y \cap T_{z,t}\big) \\
&= \begin{cases} I_{11}(s,d) + 2I_{21}(s,d) + I_{31}(s,d), & \big(0 \le s \le d/\sqrt{2}\big), \\ I_{11}(s,d) + 2I_{22}(s,d) + I_{32}(s,d), & \big(d/\sqrt{2} < s \le d\big), \\ I_{13}(s,d) + 2I_{23}(s,d) + I_{33}(s,d), & \big(d < s \le d\sqrt{2}\big), \\ I_{14}(s,d) + 2I_{24}(s,d), & \big(d\sqrt{2} < s \le \infty\big), \end{cases}
\end{aligned} \tag{C.1}$$

where

$$\begin{aligned}
I_{11}(s,d) &= \int_0^s \mathrm{d}x \int_0^x k_{sq,1}(x-y,d)\,\mathrm{d}y, \;\; (0 \le s \le d), \\
I_{13}(s,d) &= \int_0^d \mathrm{d}x \int_0^x k_{sq,1}(x-y,d)\,\mathrm{d}y + \int_d^s \mathrm{d}x \int_0^{x-d} k_{sq,2}(x-y,d)\,\mathrm{d}y \\
&\quad + \int_d^s \mathrm{d}x \int_{x-d}^x k_{sq,1}(x-y,d)\,\mathrm{d}y, \;\; \Big(d \le s \le d\sqrt{2}\Big),
\end{aligned}$$

$$
\begin{aligned}
I_{14}(s,d) &= \int_0^d \mathrm{d}x \int_0^x k_{sq,1}(x-y,d)\,\mathrm{d}y + \int_d^{d\sqrt{2}} \mathrm{d}x \int_0^{x-d} k_{sq,2}(x-y,d)\,\mathrm{d}y \\
&\quad + \int_d^{d\sqrt{2}} \mathrm{d}x \int_{x-d}^x k_{sq,1}(x-y,d)\,\mathrm{d}y + \int_{d\sqrt{2}}^s \mathrm{d}x \int_{x-d\sqrt{2}}^{x-d} k_{sq,2}(x-y,d)\,\mathrm{d}y \\
&\quad + \int_{d\sqrt{2}}^s \mathrm{d}x \int_{x-d}^x k_{sq,1}(x-y,d)\,\mathrm{d}y, \quad \Big(d\sqrt{2} \le s \le \infty\Big),
\end{aligned}
$$

$$
\begin{aligned}
I_{21}(s,d) &= \int_0^s \mathrm{d}x \int_0^x k_{sq,1}\Big(\sqrt{x^2+y^2},d\Big)\,\mathrm{d}y, \quad \Big(0 \le s \le d/\sqrt{2}\Big), \\
I_{22}(s,d) &= \int_0^{d/\sqrt{2}} \mathrm{d}x \int_0^x k_{sq,1}\Big(\sqrt{x^2+y^2},d\Big)\,\mathrm{d}y \\
&\quad + \int_{d/\sqrt{2}}^s \mathrm{d}x \int_0^{\sqrt{d^2-x^2}} k_{sq,1}\Big(\sqrt{x^2+y^2},d\Big)\,\mathrm{d}y \\
&\quad + \int_{d/\sqrt{2}}^s \mathrm{d}x \int_{\sqrt{d^2-x^2}}^x k_{sq,2}\Big(\sqrt{x^2+y^2},d\Big)\,\mathrm{d}y, \quad \Big(d/\sqrt{2} \le s \le d\Big), \\
I_{23}(s,d) &= \int_0^{d/\sqrt{2}} \mathrm{d}x \int_0^x k_{sq,1}\Big(\sqrt{x^2+y^2},d\Big)\,\mathrm{d}y \\
&\quad + \int_{d/\sqrt{2}}^d \mathrm{d}x \int_0^{\sqrt{d^2-x^2}} k_{sq,1}\Big(\sqrt{x^2+y^2},d\Big)\,\mathrm{d}y \\
&\quad + \int_{d/\sqrt{2}}^d \mathrm{d}x \int_{\sqrt{d^2-x^2}}^x k_{sq,2}\Big(\sqrt{x^2+y^2},d\Big)\,\mathrm{d}y \\
&\quad + \int_d^s \mathrm{d}x \int_0^{\sqrt{2d^2-x^2}} k_{sq,2}\Big(\sqrt{x^2+y^2},d\Big)\,\mathrm{d}y, \quad \Big(d \le s \le d\sqrt{2}\Big),
\end{aligned}
$$

$$
\begin{aligned}
I_{24}(s,d) &= \int_0^{d/\sqrt{2}} \mathrm{d}x \int_0^x k_{sq,1}\Big(\sqrt{x^2+y^2},d\Big)\,\mathrm{d}y \\
&\quad + \int_{d/\sqrt{2}}^d \mathrm{d}x \int_0^{\sqrt{d^2-x^2}} k_{sq,1}\Big(\sqrt{x^2+y^2},d\Big)\,\mathrm{d}y \\
&\quad + \int_{d/\sqrt{2}}^d \mathrm{d}x \int_{\sqrt{d^2-x^2}}^x k_{sq,2}\Big(\sqrt{x^2+y^2},d\Big)\,\mathrm{d}y \\
&\quad + \int_d^{d\sqrt{2}} \mathrm{d}x \int_0^{\sqrt{2d^2-x^2}} k_{sq,2}\Big(\sqrt{x^2+y^2},d\Big)\,\mathrm{d}y, \quad \Big(d\sqrt{2} \le s \le \infty\Big),
\end{aligned}
$$

$$
\begin{aligned}
I_{31}(s,d) &= \int_0^s \mathrm{d}x \int_0^x k_{sq,1}\Big(\sqrt{(x-y)^2+s^2}, d\Big)\,\mathrm{d}y, \quad \Big(0 \le s \le d/\sqrt{2}\Big),\\
I_{32}(s,d) &= \int_0^{\sqrt{d^2-s^2}} \mathrm{d}x \int_0^x k_{sq,1}\Big(\sqrt{(x-y)^2+s^2}, d\Big)\,\mathrm{d}y\\
&\quad + \int_{\sqrt{d^2-s^2}}^s \mathrm{d}x \int_0^{x-\sqrt{d^2-s^2}} k_{sq,2}\Big(\sqrt{(x-y)^2+s^2}, d\Big)\,\mathrm{d}y\\
&\quad + \int_{\sqrt{d^2-s^2}}^s \mathrm{d}x \int_{x-\sqrt{d^2-s^2}}^x k_{sq,1}\Big(\sqrt{(x-y)^2+s^2}, d\Big)\,\mathrm{d}y, \quad \Big(d/\sqrt{2} \le s \le d\Big),\\
I_{33}(s,d) &= \int_0^{\sqrt{2d^2-s^2}} \mathrm{d}x \int_0^x k_{sq,2}\Big(\sqrt{(x-y)^2+s^2}, d\Big)\,\mathrm{d}y\\
&\quad + \int_{\sqrt{2d^2-s^2}}^s \mathrm{d}x \int_{x-\sqrt{2d^2-s^2}}^x k_{sq,2}\Big(\sqrt{(x-y)^2+s^2}, d\Big)\,\mathrm{d}y, \quad \Big(d \le s \le d\sqrt{2}\Big).
\end{aligned}
$$

C.2 **Square hit by the vertices of another square**

Here we display the necessary expressions to compute $\mathbb{E}\widehat{\nu}_2^2\big(Y, T^{(0)}\big)$, see the first Eq, (5.16), for the corresponding plot of Fig. 9. The probe $T^{(0)}$ is the union of the four vertices of a square of diagonal length l hitting a square of side length d uniformly and isotropically at random. The procedure is analogous to that for the disk, see Eq. (3.20). Thus,

$$
\begin{aligned}
&\frac{1}{4}\,\mathbb{E}_t\nu_2\big(Y \oplus \breve{T}_{0,t}\big)\,\mathbb{E}\nu_0^2(Y \cap T_{z,t})\\
&\qquad = \begin{cases}
d^2 + 2k_{sq,1}\big(l/\sqrt{2}, d\big) + k_{sq,1}(l,d), & (0 \le l \le d),\\
d^2 + 2k_{sq,1}\big(l/\sqrt{2}, d\big) + k_{sq,2}(l,d), & \big(d < l \le d\sqrt{2}\big),\\
d^2 + 2k_{sq,2}\big(l/\sqrt{2}, d\big), & \big(d\sqrt{2} < l \le 2d\big),\\
d^2, & (2d < l < \infty).
\end{cases}
\end{aligned}
\tag{C.2}
$$

Appendix D. LIST OF NOTATION

- $\uparrow$: hitting event.
- $1_Y(x)$: Indicator function of a subset Y, that is $1_Y(x) = 1$ if $x \in Y$ and $1_Y(x) = 0$ otherwise. Useful properties are: (i) For a bounded set $T_x \subset \mathbb{R}^n$ with associated point x, $1_{T_x}(y) = 1_{T_{x-z}}(y-z)$. (ii) For a translation invariant integrable function $f : \mathbb{R}^n \to \mathbb{R}$, $\int_{T_x} f(y)\,\mathrm{d}y = \int_{T_0} f(y+x)\,\mathrm{d}y$.
- $\oplus$: Minkowski addition or subset addition, namely $Y \oplus T = \{y + x : y \in Y, x \in T\}$ for $Y, T \subset \mathbb{R}^n$. The subset consisting of all points x such that $T_{x,t}$ hits Y is precisely $Y \oplus \breve{T}_{0,t}$, that is, $Y \oplus \breve{T}_{0,t} = \{x : Y \cap T_{x,t} \neq \emptyset\}$.
- B_k: Unit ball in $\mathbb{R}^k$.
- $B_k(x,r)$: Ball in $\mathbb{R}^k$ with centre $x \in \mathbb{R}^k$ and radius r.

- b_k: Volume of B_k, i.e. $b_k = \nu_k(B_k) = O_{k-1}/k = \pi^{k/2}/\Gamma(k/2+1)$.
- $\mathrm{CV}^2(Z) = \mathrm{Var}(Z)/(\mathbb{E}Z)^2$, square coefficient of variation of the random variable Z.
- ∂Y: Boundary of the set Y.
- $\dim(Y)$: dimension of the manifold Y.
- $\mathrm{d}L_{q[0]}$: invariant density on $G_{q,n-q}$.
- $\mathrm{d}L_q$: invariant density on $F_{n,q}$.
- $\mathbb{E}Z$: mean value, or mathematical expectation, of the random variable Z.
- $F_{n,q}$: space of $q-$dimensional affine linear subspaces or $q-$flats.
- FUR: uniform random of fixed orientation.
- $G_{q,n-q}$: Grassmann manifold, space of non oriented linear $q-$subspaces in $\mathbb{R}^n$.
- G_n: special group of motions in $\mathbb{R}^n$.
- $G_{n[x]}$: special group of rotations in $\mathbb{R}^n$ about a fixed point $x \in \mathbb{R}^n$, (isomorphic with the group $SO(n)$).
- IUR: isotropic and uniform random.
- $J_{0,t}$: fundamental tile of a partition of $\mathbb{R}^n$, with an associated point at the origin and orientation $t \in G_{n[x]}$.
- $\Lambda_{x,t}$: test system of bounded $q-$probes, or of $q-$flats.
- $L_q \equiv L_q(z,t)$: $q-$dimensional linear affine subspace in $\mathbb{R}^n$ with orientation $t \in G_{q,n-q}$ and translation $z \in \mathbb{R}^{n-q}$.
- $L_{q[0]} \equiv L_q(0,t)$: $q-$dimensional linear subspace in $\mathbb{R}^n$ with orientation $t \in G_{q,n-q}$.
- $\mu(\cdot)$: kinematic measure, namely the invariant measure on G_n.
- $\mu_{[x]}(\cdot)$: invariant measure on $G_{n[x]}$.
- $\mu_q(\cdot)$: invariant measure on $F_{n,q}$.
- $\nu_q(\cdot)$: $q-$dimensional volume measure in $\mathbb{R}^n$ (Hausdorff measure).
- O_k: surface area of $\mathbb{S}^k$, i.e., $\nu_k\left(\mathbb{S}^k\right) = 2\pi^{(k+1)/2}/\Gamma((k+1)/2)$.
- $\mathbb{P}(\cdot)$: probability measure.
- $\mathbb{P}(\mathrm{d}x)$: probability element, namely the probability that a random variable takes a value in an infinitesimal neighbourhood of x. If $f(\cdot)$ is the density, then $\mathbb{P}(\mathrm{d}x) = f(x)\,\mathrm{d}x$.
- $\mathbb{R}^k$: $k-$dimensional Euclidean space.
- $\mathbb{S}^k$: $k-$dimensional unit sphere.
- $\tau_{k,t}$: translation vector.
- $T_{x,t}$: bounded $q-$dimensional probe with associated point x and orientation t.

- $\breve{T}_{0,t}$: symmetric of $T_{0,t}$ with respect to the origin, namely $\breve{T}_{0,t} \equiv -T_{0,t} = \{-x : x \in T_{0,t}\}$.
- $\mathrm{Var}(Z) = \mathbb{E}Z^2 - \big(\mathbb{E}Z\big)^2$, variance of a random variable Z.
- Y_t': orthogonal projection of a set $Y \subset \mathbb{R}^n$ onto $L_{n-q}(0,t)$.